HOLOGRAPHIC SKYRMIONS

PAUL SUTCLIFFE

Department of Mathematical Sciences, Durham University, Durham DH1 3LE, U.K.

p.m.sutcliffe@durham.ac.uk

Skyrmions are topological solitons that describe baryons within a nonlinear theory of pions. In holographic QCD, baryons correspond to topological solitons in a bulk theory with an extra spatial dimension: thus the three-dimensional Skyrmion lifts to a four-dimensional holographic Skyrmion in the bulk. We begin this review with a description of the simplest example of this correspondence, where the holographic Skyrmion is exactly the self-dual Yang-Mills instanton in flat space. This places an old result of Atiyah and Manton within a holographic framework and reveals that the associated Skyrme model extends the nonlinear pion theory to include an infinite tower of vector mesons, with specific couplings for a BPS theory. We then describe the more complicated curved space version that arises from the string theory construction of Sakai and Sugimoto. The basic concepts remain the same but the technical difficulty increases as the holographic Skyrmion is a curved space version of the Yang-Mills instanton, so self-duality and integrability are lost. Finally, we turn to a low-dimensional analogue of holographic Skyrmions, where aspects such as multi-baryons and finite baryon density are amenable to both numerical computation and an approximate analytic treatment.

1. Introduction

Skyrmions[1] are topological solitons[2] that describe baryons within an effective nonlinear theory of pions, obtained from QCD in the limit of a large number of colours[3]. It is an ambitious goal to accurately capture the properties of nuclei in terms of Skyrmions, given that the energy and length units are the only free parameters of the theory. There are several aspects of nuclei that are reproduced remarkably well by the Skyrme model (for a review see Ref. 4), but there is only limited success regarding the important subject of nuclear masses. The main issue is that Skyrmions are too tightly bound in comparison to the experimental data for nuclei. The binding energy of nuclei are typically of the order of 1% of the nucleon mass, however, in the Skyrme model binding energies are an order of magnitude greater than this[5].

Pions, being the lightest mesons, are the basic fields in the Skyrme model. Restricting to a theory of pions and ignoring all other mesons is one possible reason why Skyrmions are too tightly bound and one might hope that a more comprehensive treatment could resolve this problem. Skyrme models including the ρ meson have been the subject of considerable study in the past[6,7,8,9,10] but there are difficulties because of the large number of coupling constants that need to be determined. In addition, the introduction of a number of extra unknown parameters reduces the

predictability of the Skyrme model and is contrary to the central philosophy of the Skyrmion approach to nuclei.

Holographic Skyrmions provide a new and elegant way to incorporate additional mesons without the introduction of new parameters, by packaging all the mesons together into a gauge potential in a theory with one extra space dimension. This holographic formalism can be used in two ways. The first is by unpacking the mesons through dimensional deconstruction and studying the three-dimensional Skyrmion in the theory of pions with vector mesons. The second approach is to work directly with the four-dimensional holographic Skyrmion and calculate its properties within the bulk theory. In this review we shall describe both approaches, the first for a simple flat space holographic theory and the second for the more complicated curved space holographic theory derived by Sakai and Sugimoto[11] via a string theory D-brane construction.

In the simple flat space theory the holographic Skyrmion is exactly the self-dual Yang-Mills instanton, setting an old result of Atiyah and Manton[12] within a holographic framework. Unpacking the Yang-Mills theory generates a BPS Skyrme model in which the pions are coupled to an infinite tower of vector mesons. All binding energies vanish in the BPS Skyrme model, so we see that the introduction of the vector mesons has indeed reduced the Skyrmion binding energies. In fact, the infinite tower of vector mesons has done the job too well and has completely eliminated all binding energies. By truncating to a finite tower of vector mesons, small binding energies can be retained, but at a much lower level than in the theory with pions alone. This is precisely the situation that is required to improve the comparison with experimental binding energies and we shall discuss the progress made so far in this direction.

Computing four-dimensional holographic Skyrmions in curved space is a significant numerical challenge and only recently has this been achieved[13] for the case of a single holographic Skyrmion in the model derived by Sakai and Sugimoto. This numerical result is presented together with a comparison to earlier analytic approximations. It turns out that even the tail behaviour of the holographic Skyrmion is subtle and yields an unexpected result that can be understood analytically and confirmed numerically. Multi-baryons and the system at finite baryon density are currently beyond numerical field theory computations. Various approximations have been applied to investigate these important issues and have led to proposals for finite density configurations that include dyonic salt[14] and baryonic popcorn[15,16]. It is possible to get an improved understanding of these aspects by studying a low-dimensional toy version of this problem[17], where the holographic Skyrmion is two-dimensional. This toy model will be reviewed, together with the analytic and numerical results that, in particular, reveal analogues of both dyonic salt and baryonic popcorn.

Finally, in the conclusion we discuss some open problems and directions for future research within the topic of holographic Skyrmions.

2. Skyrmions and instantons

In the Skyrme model[1] the pion degrees of freedom are encoded into an $SU(2)$-valued Skyrme field U, and the static energy can be written in terms of the $su(2)-$valued current $R_i = \partial_i U\, U^{-1}$, where $i = 1, 2, 3$ runs over the three spatial dimensions of $\mathbb{R}^3$. In the massless pion approximation, the static energy of the Skyrme model is

$$E_S = \int \left(-\frac{c_1}{2}\mathrm{Tr}(R_i R_i) - \frac{c_2}{16}\mathrm{Tr}([R_i, R_j]^2) \right) d^3x, \tag{1}$$

where we use dimensionless units and the constants c_1 and c_2 simply set the energy and length scales. The physical energy and length units are to be fixed by comparison with experimental data. As the Skyrme model is an approximate effective theory with only two parameters, there are a variety of ways in which to fit these two parameters to the wealth of experimental results. These include fitting to meson properties, such as the pion decay constant, or properties of a single nucleon and its excited states, or to nuclei with baryon number greater than one. These different approaches yield slightly different physical energy and length units, but most of the issues discussed in this review are independent of the choice of these physical units, so we shall not need to address this aspect.

The Skyrme field is required to tend to the identity matrix at spatial infinity and this compactifies space to S^3. A given Skyrme field therefore has an associated integer topological charge $B \in \mathbb{Z} = \pi_3(SU(2))$ given explicitly by

$$B = -\frac{1}{24\pi^2}\int \varepsilon_{ijk}\mathrm{Tr}(R_i R_j R_k)\, d^3x. \tag{2}$$

It is this topological charge that is to be identified with baryon number[3]. The Skyrmion of charge B is the global minimum of the energy (1) for all fields in the given topological charge sector.

Skyrme units are often used, which corresponds to setting $c_1 = c_2 = 1$, but in the general form (1) the Faddeev-Bogomolny energy bound[18] reads

$$E_{\mathrm{S}} \geq 12\pi^2\sqrt{c_1 c_2}\,|B|. \tag{3}$$

It is easy to prove that this bound cannot be attained for non-zero B and therefore, in this sense, Skyrmions are not BPS solitons. The 1-Skyrmion is spherically symmetric and the Skyrme field has the hedgehog form

$$U = \exp(if(r)\sigma_i x_i/r), \tag{4}$$

where σ_i are the Pauli matrices and $f(r)$ is a real radial profile with the boundary conditions $f(0) = \pi$ and $f(\infty) = 0$. This profile function can only be obtained numerically, for example by substituting the ansatz (4) into the energy (1) and performing a minimization computation. This yields the result that the 1-Skyrmion energy exceeds the above bound by 23%.

Numerical Skyrmion solutions have been obtained up to reasonably large baryon numbers[5] and baryon density isosurfaces for Skyrmions with baryon numbers one to

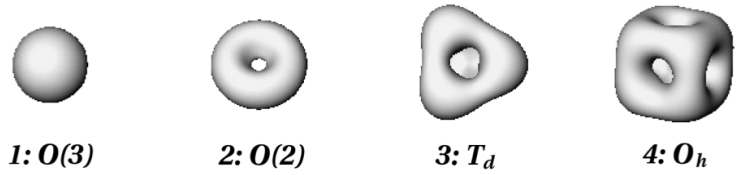

Fig. 1. Baryon density isosurfaces for Skyrmions with baryon number one to four.

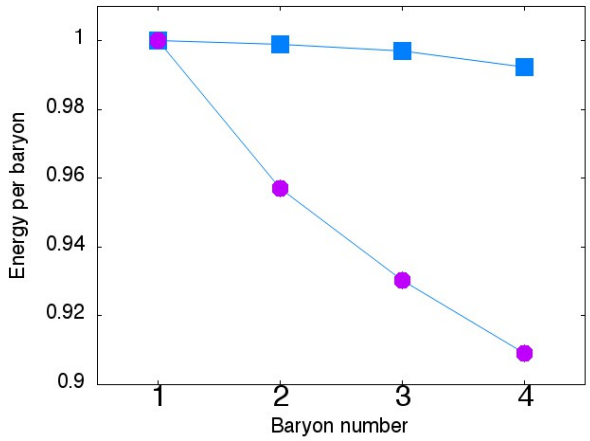

Fig. 2. The energy per baryon, in units of the single baryon energy, for baryon numbers one to four. Squares are the experimental data for nuclei and circles are Skyrmion energies.

four are displayed in Figure 1. Only the 1-Skyrmion is spherically symmetric, with the 2-Skyrmion having an axial symmetry. The 3-Skyrmion and 4-Skyrmion have only discrete symmetries, being tetrahedrally and cubically symmetric respectively. The circles in Figure 2 denote the energy per Skyrmion of these four Skyrmions, in units of the 1-Skyrmion energy to make this plot independent of the choice of units. For comparison, the squares in Figure 2 represent the experimental ground state energies per baryon for the deuteron ^{2}H, the isospin doublet ^{3}H/^{3}He and the α-particle ^{4}He, in units of the nucleon mass.

This figure provides a clear illustration of the Skyrmion binding energy problem mentioned in the introduction. As the baryon number increases there is a significant decrease in the Skyrmion energy per baryon, compared to the experimental data, reflecting the fact that Skyrmions are too tightly bound. The heart of the problem lies in the fact that the single Skyrmion exceeds the energy bound by the considerable amount of 23%, which leaves plenty of room for significant binding energies for Skyrmions with larger baryon numbers.

The solution of the Skyrme model that gets closest to the bound (3) is the infinite triply periodic Skyrme crystal[19,20], which exceeds the bound by less than 4%. This

is a crystal of half-Skyrmions and may be thought of as formed by a cubic stacking of the cubic 4-Skyrmion displayed in the final image of Figure 1. The half-Skyrmion structure is already apparent in the 4-Skyrmion, with the baryon density localized around the eight vertices of the cube. The difference between the 23% excess of the single Skyrmion and the 4% excess of the Skyrme crystal demonstrates the scale of the binding energy problem. It is expected that Skyrmions with large baryon numbers resemble finite chunks of the Skyrme crystal and this has been studied in some detail recently for the case of massive pions[21].

The antecedent to a holographic description of Skyrmions is the work of Atiyah and Manton[12], who introduced a procedure to construct Skyrme fields from the holonomy of an $SU(2)$ Yang-Mills instanton in $\mathbb{R}^4$. In the remainder of this section, we briefly review this construction.

Consider an $SU(2)$ Yang-Mills theory in four-dimensional Euclidean space. Our notation is that uppercase latin indices run over all four space coordinates x_I, with $I = 1, 2, 3, 4$. To make contact with the holographic formalism used later, we shall single out the fourth spatial direction and write $x_4 = z$. The Cartesian coordinates in the remaining $\mathbb{R}^3 \subset \mathbb{R}^4$ are denoted by $\mathbf{x} = (x_1, x_2, x_3)$, and we use lowercase latin indices (excluding z) for these components, that is, x_i with $i = 1, 2, 3$.

Let A_I be the $su(2)$-valued components of the gauge potential of the Yang-Mills theory defined by the energy

$$E_{\rm YM} = -\frac{1}{8}\int {\rm Tr}(F_{IJ}F_{IJ})\, d^3x\, dz, \tag{5}$$

where $F_{IJ} = \partial_I A_J - \partial_J A_I + [A_I, A_J]$ and the factor of $\frac{1}{8}$ is due to the normalization of the $su(2)$ generators as $-{\rm Tr}(T_a T_b) = 2\delta_{ab}$. There is a lower bound on the energy

$$E_{\rm YM} \geq 2\pi^2\, |N|, \tag{6}$$

in terms of the instanton number of the gauge field

$$N = -\frac{1}{16\pi^2}\int {\rm Tr}(F_{IJ}\, {}^\star F_{IJ})\, d^3x\, dz, \tag{7}$$

where ${}^\star F_{IJ} = \frac{1}{2}\varepsilon_{IJKL}F_{KL}$ is the dual field strength.

Unlike the Skyrme model, this is a BPS theory, in that the lower bound is attained by self-dual instantons that satisfy ${}^\star F_{IJ} = F_{IJ}$. There is an $8N$-dimensional moduli space of self-dual N-instantons and, roughly speaking, the $8N$ parameters correspond to each of the N instantons having an arbitrary position in $\mathbb{R}^4$, an arbitrary $SU(2)$ global phase and an arbitrary size associated with the conformal invariance of the theory. The integrability of the self-dual Yang-Mills equation provides a mechanism, the ADHM construction[22], that transforms the problem of calculating instanton solutions into a purely algebraic problem. In principle this provides a method to obtain the arbitrary $8N$-parameter instanton solution for all N and in practice it allows the explicit construction of a large class of instantons.

The simplest example of a self-dual instanton is the $SO(4)$ symmetric 1-instanton positioned at the origin. It is given by the simple explicit solution

$$A_I = -\frac{i\sigma_{IJ}x_J}{\rho^2+\mu^2}, \tag{8}$$

where μ is the arbitrary size of the instanton, ρ is the four-dimensional radius

$$\rho = \sqrt{x_1^2+x_2^2+x_3^2+z^2}, \tag{9}$$

and σ_{IJ} is the anti-symmetric 't Hooft tensor, defined in terms of the Paul matrices by

$$\sigma_{ij} = \varepsilon_{ijk}\sigma_k, \qquad \sigma_{zi} = \sigma_i. \tag{10}$$

The Atiyah-Manton prescription to obtain a Skyrme field from an instanton is to compute the holonomy of the instanton along lines parallel to the z-axis. Explicitly,

$$U(\mathbf{x}) = \mathcal{P}\exp\int_{-\infty}^{\infty} A_z(\mathbf{x},z)\,dz, \tag{11}$$

where $\mathcal{P}$ denotes path ordering. As A_z takes values in the Lie algebra $su(2)$ its exponential is group-valued, so that $U(\mathbf{x}) : \mathbb{R}^3 \mapsto SU(2)$, as required for a static Skyrme field. As shown by Atiyah and Manton[12], the baryon number of this Skyrme field is equal to the instanton number of the gauge field, that is, $B = N$, where these two quantities are given by (2) and (7).

This construction does not provide any exact solutions of the Skyrme model, but for each N a suitable choice of instanton, including its size, provides a remarkably good approximation to the static Skyrmion with baryon number N. The energy of the best instanton generated Skyrme field is typically around a percent higher than that of the true Skyrmion solution and correctly reproduces the symmetry of the Skyrmion for a range of highly symmetric cases studied to date.

An elementary example is provided by considering the case $N = 1$. Computing the holonomy (11) of the 1-instanton (8) generates a Skyrme field of the hedgehog form (4) with the explicit profile function

$$f(r) = \pi\left[1 - \frac{r}{\sqrt{r^2+\mu^2}}\right]. \tag{12}$$

The Skyrme energy (1) of this field depends on the instanton size μ, and is minimal for a particular finite size at which the energy is 24% above the bound (3), hence only 1% greater than the true 1-Skyrmion energy.

Instantons have been constructed with holonomies that provide good approximations to the Skyrmions displayed in Figure 1 with spherical, axial, tetrahedral and cubic symmetry[12,23]. A detailed study of the imposition of instanton symmetries within the ADHM construction has been performed and symmetric instantons obtained that describe Skyrmions with larger baryon numbers[24,25]. The Skyrmions from instantons scheme also gives an approximation to the Skyrme crystal, as the holonomy of an instanton on the four-torus[26]. Unfortunately there is no known

explicit expression for the relevant periodic instanton or Skyrme field, despite the integrability of the self-dual Yang-Mills equation.

In the following section we place the Atiyah-Manton construction of Skyrme fields from self-dual instanton holonomies within the framework of flat space holography.

3. Skyrme models from flat space holography

In holographic approaches, a QCD-like theory has a dual description as a boundary theory of an effective Yang-Mills bulk system in a curved space with an additional holographic space dimension. The meson content of the boundary theory is obtained by expanding the gauge potential in terms of Kaluza-Klein modes in the holographic direction. In flat Euclidean space a similar approach is possible[27] by replacing the Kaluza-Klein modes by Hermite functions, as we now review.

For non-negative integer n, the Hermite functions are given by

$$\psi_n(z) = \frac{(-1)^n}{\sqrt{n!\,2^n\sqrt{\pi}}} e^{\frac{1}{2}z^2} \frac{d^n}{dz^n} e^{-z^2}, \tag{13}$$

and satisfy the decay conditions $\psi_n(\pm\infty) = 0$, together with the orthonormality relation

$$\int_{-\infty}^{\infty} \psi_m(z)\psi_n(z)\, dz = \delta_{mn}. \tag{14}$$

Denoting differentiation with respect to z by a prime, then

$$\psi_n'(z) = \sqrt{\frac{n}{2}}\psi_{n-1}(z) - \sqrt{\frac{n+1}{2}}\psi_{n+1}(z), \tag{15}$$

which implies that

$$\int_{-\infty}^{z} \psi_{2p+1}(\xi)\, d\xi = \sum_{m=0}^{p} \gamma_{2p+1}^m\, \psi_{2m}(z), \tag{16}$$

$$\int_{-\infty}^{z} \psi_{2p}(\xi)\, d\xi = \gamma_{2p}^+\, \psi_+(z) + \sum_{m=0}^{p-1} \gamma_{2p}^m\, \psi_{2m+1}(z), \tag{17}$$

where γ_{2p}^+ and γ_n^m are non-zero constants.

The additional kink function $\psi_+(z)$ that appears above is defined by

$$\psi_+(z) = \frac{1}{\sqrt{2}\pi^{\frac{1}{4}}} \int_{-\infty}^{z} \psi_0(\xi)\, d\xi = \frac{1}{2} + \frac{1}{2}\mathrm{erf}(z/\sqrt{2}), \tag{18}$$

with $\mathrm{erf}(z)$ the usual error function

$$\mathrm{erf}(z) = \frac{2}{\sqrt{\pi}} \int_0^z e^{-\xi^2}\, d\xi. \tag{19}$$

The normalization of $\psi_+(z)$ has been chosen so that $\psi_+(-\infty) = 0$ and $\psi_+(\infty) = 1$.

The starting point for the flat space holographic formalism is to consider the Yang-Mills energy (5) in flat four-dimensional Eucliden space. In a gauge in which $A_I \to 0$ as $|z| \to \infty$, the components of the gauge potential can be expanded in terms of the Hermite functions $\psi_n(z)$. The gauge $A_z = 0$ is obtained by applying the gauge transformation

$$A_I \mapsto G A_I G^{-1} - \partial_I G\, G^{-1} \quad \text{with} \quad G(\mathbf{x}, z) = \mathcal{P} \exp \int_{-\infty}^{z} A_z(\mathbf{x}, \xi)\, d\xi. \tag{20}$$

The Skyrme field that describes the pion degrees of freedom is again given by the holonomy (11), and hence $U(\mathbf{x}) = G(\mathbf{x}, \infty)$. In the gauge $A_z = 0$ this holonomy appears in the boundary condition for A_i, since now $A_i \to -\partial_i U\, U^{-1}$ as $z \to \infty$.

The integral relations (16) and (17) imply that in the gauge $A_z = 0$ the remaining non-zero components of the gauge field can be expanded in terms of Hermite functions and the kink function in the form

$$A_i = -\partial_i U\, U^{-1}\, \psi_+(z) + \sum_{n=0}^{\infty} Q_i^n(\mathbf{x})\, \psi_n(z), \tag{21}$$

where the $Q_i^n(\mathbf{x})$ represent an infinite tower of vector mesons in the three-dimensional theory. The parity of the Hermite functions, $\psi_n(-z) = (-1)^n \psi(z)$, implies that for n odd the fields Q_i^n describe axial vector mesons.

The emergence of the Skyrme model of pions can be seen by neglecting all the vector fields Q_i^n. With this truncation the components of the field strength are

$$F_{zi} = -\partial_i U\, U^{-1}\, \psi_+' = -R_i \frac{\psi_0}{\sqrt{2}\pi^{\frac{1}{4}}}, \qquad F_{ij} = [R_i, R_j]\psi_+(\psi_+ - 1). \tag{22}$$

Substituting these expressions into the Yang-Mills energy $E_{\rm YM}$ given by (5), and performing the integration over z, yields precisely the Skyrme energy $E_{\rm S}$ in the form (1) where

$$c_1 = \frac{1}{4\sqrt{\pi}} = 0.141, \qquad c_2 = \int_{-\infty}^{\infty} 2\psi_+^2(\psi_+ - 1)^2\, dz = 0.198. \tag{23}$$

With these constants the Faddeev-Bogomolny energy bound (3) becomes

$$E_{\rm S} \geq 2.005\, \pi^2\, |B|, \tag{24}$$

which is to be compared with the energy bound (6) from the full Yang-Mills theory with $N = B$. This shows that the two bounds are remarkably close, but that the Faddeev-Bogomolny bound is stricter by $\frac{1}{4}\%$. Of course, the Faddeev-Bogomolny bound only applies to the Skyrme model energy $E_{\rm S}$, whereas the bound (6) is equally valid if some, or indeed all, of the vector mesons are included.

The Skyrme model is not scale invariant, in contrast to the Yang-Mills theory, and hence the scale of the Skyrme model has emerged within this approach because of the truncation that ignores the tower of vector mesons.

The vector meson terms in the expansion (21) have trivial topology and therefore the holonomy term captures all the topological features of the instanton and hence

the Skyrmion. Including the infinite tower of vector mesons produces a BPS Skyrme model, with vanishing binding energies, since the model is simply equivalent to the Yang-Mills theory with its self-dual instanton solutions. In other words, the theory flows to a conformal theory as the truncation level tends to infinity.

By varying the number of vector mesons included in the truncation, an infinite sequence of Skyrme models can be generated that interpolate between the Skyrme model containing only pions and the BPS Skyrme model containing an infinite tower of mesons. By an appropriate choice of the level of the truncation it should therefore be possible to obtain a Skyrme model with binding energies of the order of 1%, as required to match to experimental data. This holographic approach to generating a Skyrme model has the significant advantage that all coupling and interaction constants are automatically determined, and in such a way that the topological energy bound given by the right hand side of (6) not only remains valid but becomes an increasingly more accurate measure of the actual Skyrmion energy.

The remainder of this section is devoted to an analysis of the extended Skyrme model obtained by the truncation that retains only the first vector meson together with the first axial vector meson. We shall see that this indeed leads to a significant reduction in Skyrmion binding energies, in comparison to the Skyrme model of pions alone. Before this, it is perhaps worth making a comment regarding the difference between the above flat space holographic approach and the more common techniques of holographic QCD, such as those described in the next section on the Sakai-Sugimoto model. In holographic QCD the curvature of the extra dimension induces a discrete spectrum and fields are then expanded in terms of the associated Kaluza-Klein modes. In flat space holography the lack of curvature means that the spectrum is continuous. The above level truncation selects a discrete spectrum without the need for curvature, and the continuous spectrum is recovered in the limit as the truncation level tends to infinity. The truncation level is therefore a surrogate for the bulk curvature in traditional holographic theories.

To generate the extended Skyrme model with a single vector meson and a single axial vector meson we truncate the expansion (21) by including only the vector fields Q_i^0 and Q_i^1 and neglecting all Q_i^n for $n \geq 2$. For notational convenience we write $Q_i^0 = V_i$, which represents the lightest vector meson, namely the ρ meson, and write $Q_i^1 = W_i$ for the lightest axial vector meson, to be identified physically with the a_1 meson. This truncation of the expansion (21) therefore reads

$$A_i = -\partial_i U\, U^{-1}\, \psi_+(z) + V_i(\mathbf{x})\, \psi_0(z) + W_i(\mathbf{x})\, \psi_1(z). \tag{25}$$

Substituting (25) into the Yang-Mills energy (5) and performing the integration over z yields an extension of the standard Skyrme model to a static energy describing the interaction of pions with ρ and a_1 mesons. Explicitly, this energy has the form

$$E_{\pi\rho a_1} = E_{\rm S} + E_{\rm V} + E_{\rm W} + E_{\rm SV} + E_{\rm SW} + E_{\rm VW} + E_{\rm SVW}. \tag{26}$$

Here E_S is the Skyrme model pion energy (1), $E_{\rm V}$ is the vector meson energy

$$E_{\rm V} = \int -{\rm Tr}\Big\{\frac{1}{8}(\partial_i V_j - \partial_j V_i)^2 + \frac{1}{4}m^2 V_i^2 + c_3(\partial_i V_j - \partial_j V_i)[V_i, V_j] + c_4[V_i, V_j]^2\Big\}\, d^3x, \tag{27}$$

and $E_{\rm W}$ is the axial vector meson energy

$$E_{\rm W} = \int -{\rm Tr}\Big\{\frac{1}{8}(\partial_i W_j - \partial_j W_i)^2 + \frac{1}{4}M^2 W_i^2 + \frac{3}{4}c_4[W_i, W_j]^2\Big\}\, d^3x. \tag{28}$$

A crucial feature of the holographic construction of extended Skyrme models is the fact that no additional free parameters are introduced. All the new constants that appear in the energy $E_{\pi\rho a_1}$ have specific values determined by the integration over z. This includes the dimensionless ρ meson mass $m = 1/\sqrt{2}$ in (27) and the dimensionless a_1 meson mass $M = \sqrt{3/2}$ in (28). The dimensionful masses of the particles in the theory depend upon the choice of energy and length units, as discussed earlier. However, the ratio of the mass of the lightest axial vector meson to the mass of the lightest vector meson is independent of the choice of units. From the values given above this mass ratio is

$$\frac{M}{m} = \sqrt{3} = 1.73, \tag{29}$$

to be compared with the experimental result

$$\frac{m_{a_1}}{m_\rho} = \frac{1230\,{\rm MeV}}{776\,{\rm MeV}} = 1.59, \tag{30}$$

for the ratio of the a_1 to ρ mass. Given that this ratio is completely determined in the extended theory, with no adjustable parameters, then an error of less than 9% is remarkable.

The two constants c_3 and c_4 in (27) and (28) are

$$c_3 = \int_{-\infty}^{\infty} \frac{1}{4}\psi_0^3\, dz = \frac{1}{2\sqrt{6}\pi^{\frac{1}{4}}} = 0.153, \qquad c_4 = \int_{-\infty}^{\infty} \frac{1}{8}\psi_0^4\, dz = \frac{1}{8}\sqrt{\frac{1}{2\pi}} = 0.050. \tag{31}$$

The remaining terms in the energy expression (26) describe the interactions between the pions and the vector mesons. They are rather cumbersome, containing many terms, and are given by

$$\begin{aligned} E_{\rm SV} = \int -{\rm Tr}\Big\{ & c_5([R_i, V_j] - [R_j, V_i])^2 - c_6[R_i, R_j](\partial_i V_j - \partial_j V_i) - c_7[R_i, R_j][V_i, V_j] \\ & + \frac{1}{2}c_6[R_i, R_j]([R_i, V_j] - [R_j, V_i]) - \frac{1}{8}([R_i, V_j] - [R_j, V_i])(\partial_i V_j - \partial_j V_i) \\ & - \frac{1}{2}c_3([R_i, V_j] - [R_j, V_i])[V_i, V_j]\Big\}\, d^3x, \end{aligned} \tag{32}$$

$$E_{\rm SW} = \int -{\rm Tr}\Big\{ c_8([R_i,W_j]-[R_j,W_i])^2 - c_9[R_i,R_j][W_i,W_j]$$
$$+c_{10}[R_i,R_j]([R_i,W_j]-[R_j,W_i]) - \frac{1}{8}([R_i,W_j]-[R_j,W_i])(\partial_i W_j - \partial_j W_i)$$
$$-c_{11}([R_i,W_j]-[R_j,W_i])[W_i,W_j] - c_{12}R_iW_i\Big\}\, d^3x, \tag{33}$$

$$E_{\rm VW} = \int -{\rm Tr}\Big\{ \frac{1}{2}c_4([V_i,W_j]-[V_j,W_i])^2 + c_4[V_i,V_j][W_i,W_j]$$
$$+\frac{2}{3}c_3([V_i,W_j]-[V_j,W_i])(\partial_i W_j - \partial_j W_i) \tag{34}$$
$$+\frac{2}{3}c_3([W_i,W_j]-[W_j,W_i])(\partial_i V_j - \partial_j V_i)\Big\}\, d^3x,$$

and finally

$$E_{\rm SVW} = \int -{\rm Tr}\Big\{ -\frac{6}{11}c_{11}[V_i,V_j]([R_i,W_j]-[R_j,W_i])$$
$$-c_{13}([R_i,V_j]-[R_j,V_i])(\partial_i W_j - \partial_j W_i)$$
$$-c_{13}([R_i,W_j]-[R_j,W_i])(\partial_i V_j - \partial_j V_i) - \frac{1}{3}c_3[W_i,W_j]([R_i,V_j]-[R_j,V_i])$$
$$+c_{13}([R_i,V_j]-[R_j,V_i])([R_i,W_j]-[R_j,W_i])$$
$$-\frac{6}{11}c_{11}([R_i,V_j]-[R_j,V_i])([V_i,W_j]-[V_j,W_i])$$
$$-\frac{1}{3}c_3([R_i,W_j]-[R_j,W_i])([V_i,W_j]-[V_j,W_i])\Big\}\, d^3x. \tag{35}$$

These lengthy expressions illustrate the inherent difficulty in extending the Skyrme model of pions to include other mesons. Even at this order, there are a large number of interaction terms with coupling constants that must be determined. The beauty of a holographic approach to this problem is that all the coupling constants are fixed without the introduction of any new parameters. In particular, the constants $c_5,\ldots,c_{13}$ that appear in the above interaction terms are given by

$$c_5 = \int_{-\infty}^{\infty} \frac{1}{8}\psi_+^2\psi_0^2\, dz = 0.038, \quad c_6 = \int_{-\infty}^{\infty} \frac{1}{4}\psi_+(1-\psi_+)\psi_0\, dz = \frac{\pi^{1/4}}{12\sqrt{2}} = 0.078,$$
$$c_7 = \int_{-\infty}^{\infty} \frac{1}{4}\psi_+(1-\psi_+)\psi_0^2\, dz = 0.049, \quad c_8 = \int_{-\infty}^{\infty} \frac{1}{8}\psi_+^2\psi_1^2\, dz = 0.047,$$
$$c_9 = \int_{-\infty}^{\infty} \frac{1}{4}\psi_+(1-\psi_+)\psi_1^2\, dz = 0.030, \quad c_{10} = \int_{-\infty}^{\infty} \frac{1}{4}\psi_+(1-\psi_+)\psi_1\, dz = 0.016,$$
$$c_{11} = \int_{-\infty}^{\infty} \frac{1}{4}\psi_+\psi_1^3\, dz = \frac{11\sqrt{2}}{144\pi^{3/4}} = 0.046, \quad c_{12} = \frac{1}{4\pi^{1/4}} = 0.188,$$
$$c_{13} = \int_{-\infty}^{\infty} \frac{1}{4}\psi_+\psi_0\psi_1\, dz = \frac{1}{4\sqrt{6\pi}} = 0.058. \tag{36}$$

As a field of the form (25) is simply a particular subclass of field configurations with instanton number $N = B$ then the Yang-Mills energy bound (6) is applicable and provides the lower bound

$$E_{\pi\rho a_1} \geq 2\pi^2 B. \tag{37}$$

The holographically generated coupling constants are delicately balanced to yield this energy bound and it is difficult to see how one might derive this bound directly from the energy expression (26), if the holographic origin of this model was unknown.

Imposing spherical symmetry allows a numerical computation of the 1-Skyrmion solution in the extended model, with the result[27] that the energy $E_{\pi\rho a_1}$ exceeds the bound (37) by less than 5%. Thus, as anticipated, this extension of the Skyrme model moves the theory closer to a BPS theory and places a more significant restriction on the magnitude of multi-Skyrmion binding energies.

It is possible to extend the Atiyah-Manton holonomy construction to approximate static multi-Skyrmions in the extended model, as follows. Given the fields $A_i(\mathbf{x}, z)$ of an appropriate self-dual instanton in the gauge $A_z = 0$, a comparison with the expansion (25) allows the extraction of the Skyrme field currents via $R_i(\mathbf{x}) = -A_i(\mathbf{x}, \infty)$. The orthogonality of the Hermite functions then provides the following integral expressions for the vector meson fields

$$\begin{aligned} V_i(\mathbf{x}) &= \int_{-\infty}^{\infty} \Big(A_i(\mathbf{x}, z) + R_i(\mathbf{x})\psi_+(z) \Big) \psi_0(z)\, dz \\ W_i(\mathbf{x}) &= \int_{-\infty}^{\infty} \Big(A_i(\mathbf{x}, z) + R_i(\mathbf{x})\psi_+(z) \Big) \psi_1(z)\, dz. \end{aligned} \tag{38}$$

Under the assumption that the symmetry of the charge B Skyrmion in the extended theory is the same as in the Skyrme model with only pions (which seems reasonable for $B \leq 4$), then the same four instantons with spherical, axial, tetrahedral and cubic symmetry are the appropriate instantons for charges one to four. Note, however, that the instanton sizes that minimize the energy $E_{\pi\rho a_1}$ will be different from those that minimized the energy E_S in the Skyrme model with pions alone. Using each of these instantons and performing the integrals (38) numerically, together with a minimization over the instanton size, produces the Skyrmion energy results displayed as the diamonds in Figure 3.

The results[28] displayed in this figure show that the Skyrmion energies in the extended theory are much closer to the BPS bound and hence this significantly reduces Skyrmion binding energies. Although the Skyrmions are still too tightly bound in comparison to the experimental data on nuclei, there is a significant improvement on the Skyrme model with only pions. In particular, this extended theory is able to provide a reasonable approximation to the masses of nuclei with $B = 2, 3, 4$, at the expense of overestimating the energy of the single baryon. As an illustration, if the physical energy unit is fixed by matching the energy of the $B = 4$ Skyrmion to the mass of ^{4}He then this produces the data presented in Table 1, where the experimental values measured for nuclei are also shown for comparison. It can be seen

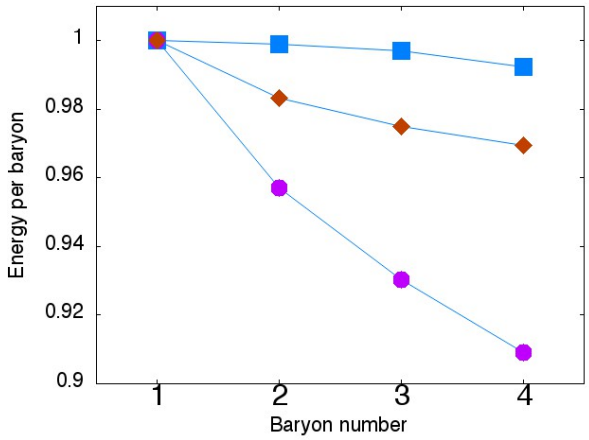

Fig. 3. The energy per baryon, in units of the single baryon energy, for baryon numbers one to four. Squares are the experimental data for nuclei, circles are the Skyrmion energies in the theory with only pions, and diamonds are the Skyrmion energies in the extended theory with pions, ρ and a_1 mesons.

that this gives a reasonable approximation to the experimental data, particularly for baryon numbers greater than one. Even the single baryon mass is only 20 MeV above the true value, whereas a similar calculation in the Skyrme model of pions gives an energy excess which is more than four times greater than this.

Table 1. For $1 \leq B \leq 4$ the experimental values of the masses of nuclei are compared with the predictions in the extended Skyrme model.

	Mass in MeV	
B	Experiment	Theory
1	939	959
2	1876	1887
3	2809	2806
4	3727	3727

It is clear from these results that extending the Skyrme model of pions to include additional mesons via a holographic approach yields encouraging signs, with binding energies dramatically reduced. Including only the lightest vector and axial vector meson already decreases the discrepencies between the values for nuclei and Skyrmions to around one quarter of those found in the Skyrme model of pions alone. By including additional vector mesons, there is hope that an accurate match to experimental data could be achieved, though this has not yet been studied due to the computational challenges induced by the large number of terms that are generated by the inclusion of each extra vector meson.

In this flat space holography approach to Skyrmions, the truncation process is vital. This is because the bulk holographic Skyrmion is simply the self-dual Yang-Mills instanton, which is BPS, and hence all binding energies vanish in the full bulk theory. For a bulk theory in a curved space the holographic Skyrmion can be similar to the Yang-Mills instanton, but self-duality and hence the BPS aspect is lost due to the curvature (and other modifications) so no truncation is required and it is possible to study the holographic Skyrmion directly in the bulk theory. This is the subject of the following section, where the bulk theory is the holographic theory of Sakai and Sugimoto[11].

4. The holographic Skyrmion in the Sakai-Sugimoto model

The Sakai-Sugimoto model[11] is a well-known example of a string theory description of holographic QCD. It is obtained by considering D8-brane probes in a background of D4-branes compactified on a circle. Here we are interested in the effective Yang-Mills-Chern-Simons theory that this generates in five-dimensional spacetime. Although the term Sakai-Sugimoto model is often used to refer to the full string theory construction, we shall continue to use this nomenclature for the effective theory too.

The cornerstone of all models of baryons in holographic QCD is that Skyrmions on the boundary correspond to solitons in the bulk, that is, to holographic Skyrmions. The Sakai-Sugimoto model differs from the flat space holographic approach of the previous section in that spacetime is curved with AdS-like behaviour and a five-dimensional Chern-Simons term is included that generates an abelian electric charge for the holographic Skyrmion. Here AdS-like means that the curvature is negative and there is a conformal boundary. Although the main contribution to the action is simply the Yang-Mills term, the combination of the curvature of spacetime and the electromagnetic repulsion provides a stability that fixes the size of the holographic Skyrmion.

In the Sakai-Sugimoto model, the validity of the supergravity approximation requires working with a large number of colours N_c and a large value of the 't Hooft coupling λ, which controls the ratio between the Yang-Mills and Chern-Simons terms. As λ is large, the holographic Skyrmion is small with respect to the curvature scale and this leads to the expectation[29,30] that the holographic Skyrmion will be well-approximated by the flat space self-dual Yang-Mills instanton with a specific small size.

In this section we first review the recent numerical results[13] that put this assumption to the test by numerically computing the holographic Skyrmion and comparing it to the self-dual instanton. We then discuss the large distance properties of the holographic Skyrmion that follow from an analysis of the fields in the tail, and reveal how this leads to the emergence of a new large scale, despite the fact that the holographic Skyrmion is considered to be small.

Consider a $(D+2)$-dimensional spacetime with a warped metric of the form

$$ds^2 = H(-dt^2 + dx_1^2 + \ldots + dx_D^2) + \frac{1}{H}dz^2, \tag{39}$$

where

$$H(z) = \left(1 + \frac{z^2}{L^2}\right)^{(D+1)/(D+3)} \tag{40}$$

The warp factor $H(z)$, multiplying the $(D+1)$-dimensional Minkowski spacetime of the dual boundary theory, depends only on the additional holographic coordinate z. The parameter L determines the curvature length scale and can be set to unity by an appropriate choice of units (although occasionally we will reintroduce L to indicate the general dependence).

The effective five-dimensional metric of the Sakai-Sugimoto model[11,31] corresponds to the choice $D = 3$, which we take for the rest of this section. In this case the spacetime has a conformal boundary as $z \to \infty$ and the scalar curvature is

$$R = -\frac{16(4z^2+3)}{9(1+z^2)^{4/3}}, \tag{41}$$

with the properties that $R \leq 0$ and R is finite (in fact zero) as $z \to \infty$. This metric is therefore AdS-like.

As in the previous section, the index notation used in this section is that uppercase indices include the holographic direction whilst lowercase indices exclude this additional dimension. Furthermore, greek indices include the time coordinate whilst latin indices (excluding z) run over the spatial coordinates. Thus, for example,

$$\Gamma, \Delta, \ldots = 0, 1, 2, 3, z, \quad I, J, \ldots = 1, 2, 3, z, \quad i, j, \ldots = 1, 2, 3. \tag{42}$$

The Sakai-Sugimoto model[11,31] is a $U(2)$ gauge theory, with anti-hermitian gauge potential $\mathcal{A}_\Gamma \in u(2)$, defined in the five-dimensional spacetime introduced above, where we denote this metric by $g_{\Gamma\Delta}$. The action is the sum of a Yang-Mills term and a $U(2)$ Chern-Simons term

$$\mathcal{S} = \frac{N_c\lambda}{54\pi^3}\int \sqrt{-g}\,\frac{1}{8}\mathrm{Tr}\left(\mathcal{F}_{\Gamma\Delta}\mathcal{F}^{\Gamma\Delta}\right)\,d^4x\,dz + \frac{N_c}{24\pi^2}\int\,\omega_5(\mathcal{A})\,d^4x\,dz. \tag{43}$$

Note that the number of colours, N_c, is simply a multiplicative factor and is therefore unimportant for the classical bulk theory.

We split the $U(2)$ gauge theory into an $SU(2)$ component and an abelian $U(1)$ component by writing

$$\mathcal{A}_\Gamma = A_\Gamma + \frac{i}{2}\widehat{A}_\Gamma, \tag{44}$$

and similarly for the gauge field. Then the $U(2)$ Chern-Simons term in (43) is (up to a total derivative) given by

$$-\frac{N_c}{24\pi^2}\int\left(\frac{3}{8}\widehat{A}_\Gamma\mathrm{Tr}\left(F_{\Delta\Sigma}F_{\Xi\Upsilon}\right) + \frac{1}{16}\widehat{A}_\Gamma\,\widehat{F}_{\Delta\Sigma}\widehat{F}_{\Xi\Upsilon}\right)\varepsilon^{\Gamma\Delta\Sigma\Xi\Upsilon}\,d^4x\,dz. \tag{45}$$

In this review we are concerned with the static solutions of the theory, hence we shall now restrict to time independent fields with $A_0 = \widehat{A}_I = 0$. In this case the abelian potential $\widehat{A}_0$ generates the electric field $\widehat{F}_{I0} = \partial_I \widehat{A}_0$. It is convenient to write the action in units of $N_c\lambda/(54\pi^3)$, which upon restriction to the above static fields becomes

$$S = \frac{1}{8}\int \left\{ \frac{1}{H^{1/2}}\mathrm{Tr}(F_{ij}^2) + 2H^{3/2}\mathrm{Tr}(F_{iz}^2) + \frac{1}{H^{1/2}}(\partial_i \widehat{A}_0)^2 + H^{3/2}(\partial_z \widehat{A}_0)^2 \right. \\ \left. -\frac{2}{\Lambda}\widehat{A}_0 \ \mathrm{Tr}\left(F_{IJ}F_{KL}\right)\varepsilon_{IJKL} \right\} d^4x\, dz, \tag{46}$$

where we have introduced the rescaled 't Hooft coupling

$$\Lambda = \frac{8\lambda}{27\pi}. \tag{47}$$

To extract the meson physics from this theory a Kaluza-Klein expansion is performed[11], in a similar way to that described in the flat space case of the previous section, but this time using the appropriate basis functions for curved space. To obtain the basis functions we begin with the eigenfunctions $\psi^{\pm}_{(k)}(z)$, defined as the solutions to the linear equation

$$H^{1/2}\partial_z(H^{3/2}\partial_z\psi^{\pm}_{(k)}) + k^2\psi^{\pm}_{(k)} = 0, \tag{48}$$

where the superscript $^{\pm}$ refers to even and odd parity with respect to $z \to -z$. The boundary conditions for $\psi^{\pm}_{(k)}(z)$ are

$$\psi^{+}_{(k)}(0) = 1, \qquad \partial_z\psi^{+}_{(k)}(0) = 0, \qquad \psi^{-}_{(k)}(0) = 0, \qquad \partial_z\psi^{-}_{(k)}(0) = 1. \tag{49}$$

In holographic QCD, the correct holographic prescription at the conformal boundary is that there are no sources for the operators in the dual theory. This corresponds to the requirement that the parallel components the field strength vanish at the boundary $z = \pm\infty$. In terms of an eigenfunction expansion, this condition translates to the boundary condition

$$\psi^{\pm}_{(k)}(\infty) = 0, \tag{50}$$

which selects only a discrete set of momenta, k_n with $n = 1, 2, \ldots$ and $k_1 > 0$. The momenta associated with the even and odd eigenfunctions interlace and we impose the ordering $k_{n+1} > k_n$.

The odd (even) values of n correspond to even (odd) functions with respect to $z \to -z$, so a more convenient notation is to label the eigenfunctions by an integer by defining

$$\psi_{2n-1}(z) \equiv \psi^{+}_{(k_{2n-1})}(z)\ , \qquad \psi_{2n}(z) \equiv \psi^{-}_{(k_{2n})}(z)\ , \qquad n = 1, 2, \ldots \tag{51}$$

so that the information about the parity of the eigenfunction is encoded in the parity of the integer index. These eigenfunctions are orthogonal, that is, $(\psi_m, \psi_n) \propto \delta_{mn}$, with respect to the inner product

$$(\psi, \widetilde{\psi}) = \int_{-\infty}^{\infty} \frac{1}{H^{1/2}}\psi\widetilde{\psi}\, dz. \tag{52}$$

The gauge potential components $A_i(x_j, z)$ can be written as an expansion in terms of the basis functions $\psi_n(z)$, with coefficients that correspond to vector meson fields in the dimensionally reduced theory. The orthogonality condition with respect to the inner product (52) ensures that when this expansion is substituted into the action (46) the resulting integration over z yields the correct Yang-Mills form of the action for each member of the infinite tower of vector mesons. The factor of $H^{-1/2}$ in the inner product (52) matches the same factor in front of the term $\mathrm{Tr}(F_{ij}^2)$ in the action (46) in order to achieve this result.

The mass of each vector meson is proportional to the associated discrete momentum k_n, and in particular the masses of the lightest vector and axial vector mesons are calculated from $k_1 = 0.82$ and $k_2 = 1.26$. This gives[11] a ratio for the a_1 to ρ meson mass of

$$\frac{k_2}{k_1} = \frac{1.26}{0.82} = 1.54, \tag{53}$$

in excellent agreement with the experimental result (30).

The component of the gauge potential $A_z(x_j, z)$ is not written as an expansion in terms of the eigenfunctions $\psi_n(z)$, but rather in terms of the basis functions $\phi_n(z)$ defined by $\phi_n(z) = \partial_z \psi_n(z)$. These functions are orthogonal, that is, $\langle \phi_m, \phi_n \rangle \propto \delta_{mn}$ with respect to the inner product

$$\langle \phi, \widetilde{\phi} \rangle = \int_{-\infty}^{\infty} H^{3/2} \phi \widetilde{\phi}\, dz, \tag{54}$$

that contains the appropriate factor of $H^{3/2}$, in agreement with the same factor that appears in front of the term $\mathrm{Tr}(F_{iz}^2)$ in the action (46), in order to produce the correct form for the dimensionally reduced action.

This set of functions includes an additional mode, $\phi_0(z) = \partial_z \psi_0(z)$, obtained from the zero mode ($k_0 = 0$)

$$\psi_0(z) = \int_0^z \frac{1}{H(\zeta)^{3/2}}\, d\zeta = \tan^{-1} z. \tag{55}$$

Note that $\psi_0(\infty) = \frac{\pi}{2} \neq 0$, hence this mode was excluded from the earlier considerations as it does not satisfy the boundary conditions at infinity. However,

$$\phi_0(z) = \frac{1}{H(z)^{3/2}} = \frac{1}{1+z^2}, \tag{56}$$

and hence this does satisfy the boundary condition as $\phi_0(\pm\infty) = 0$.

The zero mode is associated with the massless pion and, as in the flat space holographic theory of the previous section, the Skyrme field describing pions is again given by the holonomy (11), with the baryon number B equal to the instanton number N calculated via the formula (7). In detail, in the gauge $A_z = 0$ the holonomy U appears in the boundary condition for the gauge potential A_i. In this gauge the expansion of A_i includes the current $-\partial_i U\, U^{-1}$ multiplying the function

$\psi_+(z)$ constructed from the zero mode as

$$\psi_+(z) = \frac{(2\psi_0(z)+\pi)}{2\pi}. \tag{57}$$

This function satisfies the boundary conditions $\psi_+(-\infty) = 0$ and $\psi_+(\infty) = 1$ and is the curved space analogue of the flat space kink function of the previous section denoted by the same symbol. The derivation of the nonlinear meson theory works in a similar manner to the flat space holographic theory described earlier. In particular, neglecting the infinite tower of vector mesons again yields exactly the Skyrme model of pions (1), although the normalization constants c_1 and c_2 take different values.

In the baryon sector, the holographic 1-Skyrmion is the solution with $N = B = 1$ of the static field equations that follow from the variation of the action (46). These equations are given by

$$\frac{1}{H^{1/2}} D_j F_{ji} + D_z(H^{3/2} F_{zi}) = \frac{1}{\Lambda} \varepsilon_{iJKL} F_{KL} \partial_J \widehat{A}_0 \tag{58}$$

$$H^{3/2} D_j F_{jz} = \frac{1}{\Lambda} \varepsilon_{ijk} F_{jk} \partial_i \widehat{A}_0 \tag{59}$$

$$\frac{1}{H^{1/2}} \partial_i \partial_i \widehat{A}_0 + \partial_z(H^{3/2} \partial_z \widehat{A}_0) = -\frac{1}{\Lambda} \mathrm{Tr}\,(F_{IJ} F_{KL})\, \varepsilon_{IJKL}. \tag{60}$$

Note that the Chern-Simons coupling in (46) implies that the instanton charge density sources the abelian electric field. It is this electric field that provides a counterbalance to the spacetime curvature that acts to shrink the size of the holographic Skyrmion.

The above set of coupled nonlinear partial differential equations are difficult to solve, even numerically. However, in the large Λ limit the Chern-Simons term is small and hence it resists the shrinking of the holographic Skyrmion only at a size that is smaller than the curvature scale (order one in our units). One therefore expects that, at least in the core of the holographic Skyrmion, the curvature of the metric does not have a significant influence on the fields and a flat space self-dual instanton may provide a good approximation to the holographic Skyrmion.

To address this issue in detail, consider the following rescaling[29,30],

$$\widetilde{x}_I = \sqrt{\Lambda} x_I, \qquad \widetilde{t} = t, \qquad \widetilde{A}_I = A_I/\sqrt{\Lambda}, \qquad \widetilde{\widehat{A}}_0 = \widehat{A}_0, \tag{61}$$

and define $\widetilde{H} = H(\widetilde{z}/\sqrt{\Lambda})$. Using these rescaled variables and expanding the action (46) in powers of Λ^{-1} yields

$$\begin{aligned} S = \int \Big\{ & \frac{1}{8}\mathrm{Tr}\left(\widetilde{F}_{IJ}^2\right) \\ & + \frac{1}{8\Lambda}\left(\widetilde{z}^2 \mathrm{Tr}\left(\widetilde{F}_{IJ}^2\right) - \frac{4}{3}\widetilde{z}^2 \mathrm{tr}\left(\widetilde{F}_{ij}^2\right) + (\widetilde{\partial}_I \widetilde{\widehat{A}}_0)^2 - 2\widetilde{\widehat{A}}_0\ \mathrm{Tr}\,(\widetilde{F}_{IJ}\widetilde{F}_{KL})\,\varepsilon_{IJKL}\right) \\ & + \mathcal{O}\left(\frac{1}{\Lambda^2}\right) \qquad \Big\}\, d^4\widetilde{x}\, d\widetilde{z}. \end{aligned} \tag{62}$$

The leading order term is scale invariant and is simply the Yang-Mills action in flat space, which is minimized by the self-dual instanton. The next term is of order $1/\Lambda$

and contains the size stabilizing contributions from both the abelian field and the curvature. This term defines an action on the self-dual instanton moduli space and can be used to determine the size of the instanton within this approximation.

Assuming the self-dual 1-instanton form (8) for A_I and taking the variation of the second term in (62) yields (after converting back to the original unscaled variables) a linear equation for $\widehat{A}_0$ with solution

$$\widehat{A}_0 = \frac{8(\rho^2+2\mu^2)}{\Lambda(\rho^2+\mu^2)^2}. \tag{63}$$

Substituting this field and the self-dual expression (8) into the static action and performing the integration produces the associated static energy

$$E = 2\pi^2\bigg(1+\frac{1}{6}\mu^2+\frac{64}{5\Lambda^2\mu^2}\bigg)+\mathcal{O}\bigg(\frac{1}{\Lambda^2}\bigg). \tag{64}$$

The instanton size μ is obtained by minimization of this energy, which to leading order in the large Λ limit gives the small instanton size

$$\mu = \frac{4}{\sqrt{\Lambda}}\bigg(\frac{3}{10}\bigg)^{1/4}. \tag{65}$$

We now see the various contributions to the energy and their role in determining the size of the instanton. The first term in (64) is independent of the instanton size and is simply the flat space self-dual Yang-Mills result of $2\pi^2$. The second term is $\mathcal{O}(\mu^2)$ and derives from the Yang-Mills term as the leading order correction from the metric expansion about flat space. This contribution drives the instanton towards zero size. The third term in (64) is the leading contribution from the electrostatic abelian field and being of order $\mathcal{O}(1/\mu^2)$ it resists the shrinking of the instanton size. These competing effects combine to produce the finite size (65), which is small for large Λ, with the energy dominated by the flat space self-dual contribution.

To confirm the validity of the above self-dual instanton approximation requires a numerical solution of the full nonlinear curved space partial differential equations (58)–(60), to compute the holographic 1-Skyrmion. This has recently been performed[13] and we now review this computation and the results.

Unlike the self-dual Yang-Mills 1-instanton in flat space, the fields of a static holographic 1-Skyrmion are not compatible with an $SO(4)$ spherically symmetric ansatz. However, the problem can be reduced to an effective two-dimensional computation by employing an $SO(3)$ symmetric ansatz of the form[32,33]

$$A_j = -\frac{i}{2}\bigg(\frac{1+\Phi_2}{r^2}\varepsilon_{jak}x_k+\frac{\Phi_1}{r}(\delta_{ja}-\frac{x_jx_a}{r^2})+a_r\frac{x_jx_a}{r^2}\bigg)\sigma_a, \quad A_z = -\frac{i}{2r}a_zx_a\sigma_a, \tag{66}$$

where the fields Φ_1, Φ_2, a_r, a_z and $\widehat{A}_0$ are functions of the holographic coordinate z and the three-dimensional radius $r=\sqrt{x_1^2+x_2^2+x_3^2}$.

Writing $\Phi = \Phi_1 + i\Phi_2$, $f_{rz} = \partial_r a_z - \partial_z a_r$ and $D_r\Phi = \partial_r\Phi - ia_r\Phi$, together with $D_z\Phi = \partial_z\Phi - ia_z\Phi$, the expression for the baryon number becomes

$$B = -\int_0^\infty dr\int_{-\infty}^\infty dz\ \frac{1}{2\pi}\bigg\{f_{rz}(1-|\Phi|^2)+i(D_r\Phi\overline{D_z\Phi}-\overline{D_r\Phi}D_z\Phi)\bigg\}. \tag{67}$$

In terms of these variables, the energy obtained from the action (46) has three terms, $E = \pi(E_{SU(2)} + E_{U(1)} + E_{CS})$, where

$$E_{SU(2)} = \int_0^\infty dr \int_{-\infty}^\infty dz \left\{ H^{-\frac{1}{2}} |D_r\Phi|^2 + H^{\frac{3}{2}} |D_z\Phi|^2 + \frac{r^2 H^{\frac{3}{2}}}{2} f_{rz}^2 + \frac{H^{-\frac{1}{2}}}{2r^2}(1-|\Phi|^2)^2 \right\}, \tag{68}$$

$$E_{U(1)} = -\int_0^\infty dr \int_{-\infty}^\infty dz \left\{ \frac{1}{2} r^2 \left(H^{-\frac{1}{2}} (\partial_r \widehat{A}_0)^2 + H^{\frac{3}{2}} (\partial_z \widehat{A}_0)^2 \right) \right\}, \tag{69}$$

$$E_{CS} = -\frac{1}{\Lambda} \int_0^\infty dr \int_{-\infty}^\infty dz \left\{ 4\widehat{A}_0 \left(f_{rz}(1-|\Phi|^2) + i(D_r\Phi \overline{D_z\Phi} - \overline{D_r\Phi} D_z\Phi) \right) \right\}. \tag{70}$$

For reference, in this formalism the flat space self-dual instanton is given by

$$\Phi = \frac{2rz + i(r^2 - z^2 - \mu^2)}{\rho^2 + \mu^2}, \quad a_r = \frac{2z}{\rho^2 + \mu^2}, \quad a_z = \frac{-2r}{\rho^2 + \mu^2}, \tag{71}$$

where, as earlier, $\rho^2 = r^2 + z^2$. The required soliton has $B = 1$ and is a vortex in the reduced theory on the half-plane $r \geq 0$. On the boundary $\{r = 0\} \cup \{\rho = \infty\}$ the complex field Φ has unit modulus and its phase varies by 2π around the boundary. Setting $\mu = 0$ in (71) gives the fields

$$\Phi = \frac{2rz + i(r^2 - z^2)}{\rho^2}, \qquad a_r = \frac{2z}{\rho^2}, \qquad a_z = \frac{-2r}{\rho^2}, \tag{72}$$

which are pure gauge but have a singularity at the point $\rho = 0$. These fields satisfy $|\Phi| = 1$ and $D_r\Phi = D_z\Phi = f_{rz} = 0$, which together with $\widehat{A}_0 = 0$ constitute the boundary conditions as $\rho \to \infty$. In particular, the phase of Φ varies by 2π along this boundary. The boundary conditions along the line $r = 0$ are given by $\partial_r \widehat{A}_0 = 0$ and $\Phi = -i,\ D_r\Phi = D_z\Phi = 0$, which are those of the finite size self-dual instanton.

The field equations that follow from the variation of the energy E can be solved using a heat flow method that corresponds to a constrained energy minimization, where the energy $E_{SU(2)} + E_{CS}$ is minimized subject to the constraint that $\widehat{A}_0$ satisfies the field equation

$$\frac{1}{r^2 H^{1/2}} \partial_r (r^2 \partial_r \widehat{A}_0) + \partial_z (H^{3/2} \partial_z \widehat{A}_0) = \frac{4}{\Lambda r^2} \left\{ f_{rz}(1-|\Phi|^2) + i(D_r\Phi \overline{D_z\Phi} - \overline{D_r\Phi} D_z\Phi) \right\}, \tag{73}$$

which is a curved space Poisson equation sourced by the instanton charge density.

It turns out to be computationally efficient to perform the change of variable $z = \tan w$, so that the infinite domain of z transforms to the finite interval $w \in [-\frac{\pi}{2}, \frac{\pi}{2}]$. At the boundaries $w = \pm\frac{\pi}{2}$ the fields (72) now give the boundary conditions $\Phi = -i,\ a_r = a_z = \widehat{A}_0 = 0$. The numerical solution is computed on a grid with a boundary at a finite value $r = r_\star$. The boundary conditions applied at this simulation boundary are that the fields are given by the pure gauge fields (72) together with $\widehat{A}_0 = 0$, that is,

$$\Phi = \frac{2r_\star \tan w + i(r_\star^2 - \tan^2 w)}{r_\star^2 + \tan^2 w}, \quad a_r = \frac{2\tan w}{r_\star^2 + \tan^2 w}, \quad a_z = -\frac{2r_\star}{r_\star^2 + \tan^2 w}. \tag{74}$$

Note that the 2π phase winding of Φ now takes place along the single boundary $r = r_\star$. The solutions are insensitive to the choice of this finite boundary, providing $r_\star$ is taken to be sufficiently large.

To display the results of the numerical computations it is convenient to plot the abelian potential $\widehat{A}_0$, and to compare this with the simple explicit expression (63) for $\widehat{A}_0$ within the flat space self-dual approximation.

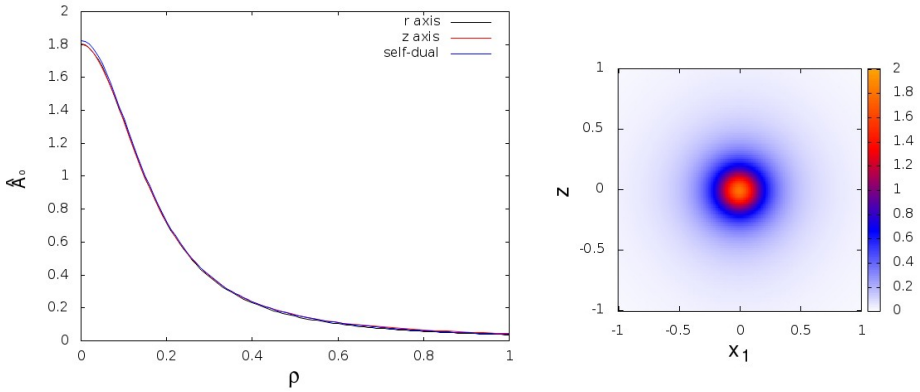

Fig. 4. The abelian potential $\widehat{A}_0$ for the holographic Skyrmion with $\Lambda = 200$. The left image displays plots of $\widehat{A}_0$ along the r-axis (black curve) and the z-axis (red curve). The flat space self-dual approximation (blue curve) is included for comparison. All three curves are almost indistinguishable as the self-dual field provides a good approximation in this range, apart from a very slight overshoot at the origin. The right image is a plot of $\widehat{A}_0$ in the plane $x_2 = x_3 = 0$ and demonstrates the approximate $SO(4)$ symmetry in this region.

Figure 4 displays a plot of $\widehat{A}_0$ for the value $\Lambda = 200$. The plot in the left image presents $\widehat{A}_0$ along the r and z axes, together with the $SO(4)$ symmetric self-dual instanton approximation (63) with the instanton size given by (65). All three curves are almost indistinguishable, which confirms that the self-dual instanton provides a good approximation in this range, for this large value of Λ. The plot in the right image presents $\widehat{A}_0$ in the plane $x_2 = x_3 = 0$, and demonstrates the approximate $SO(4)$ symmetry for $\rho \lesssim L = 1$.

To see a deviation from the self-dual approximation requires an examination of the region $\rho > L = 1$. As $\widehat{A}_0$ is small in this region then the appropriate quantity to plot is $\log \widehat{A}_0$, which is presented in Figure 5 for $0 \leq \rho \leq 3$. The lack of $SO(4)$ symmetry is now more apparent, with a slower decay along the z-axis than along the r-axis. We now review an analytic derivation of the tail behaviour of the holographic Skyrmion[13], that explains this numerical result.

It is important to note that the self-dual instanton approximation has nothing to say about the asymptotic fields of the holographic Skyrmion at large distance, because the rescaling performed in (61) involves zooming in to a scale of order $1/\sqrt{\Lambda}$.

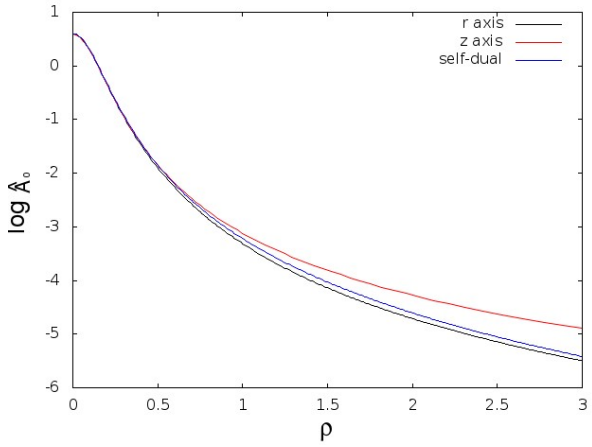

Fig. 5. For the holographic Skyrmion with $\Lambda = 200$, the plot displays $\log \widehat{A}_0$ against ρ along the r-axis (black curve) and the z-axis (red curve). The flat space self-dual approximation (blue curve) is included for comparison. There is a faster decay along the r-axis than along the z-axis.

We begin by considering a linear expansion that is valid for $L/\sqrt{\Lambda} \lesssim \rho \lesssim L$, where we recall that we have set $L = 1$. This region is far enough from the core of the holographic Skyrmion that a linear expansion is possible but is close enough to the origin that the curvature of the metric can be neglected by setting $H = 1$.

We still use $1/\Lambda$ as the small parameter of the expansion, but now we keep the length scale fixed rather than zooming in to the core. We write the expansion as

$$A_I = A_I^{(1)} + A_I^{(2)} + \dots, \qquad \widehat{A}_0 = \widehat{A}_0^{(1)} + \widehat{A}_0^{(2)} + \dots \tag{75}$$

in which

$$A_I^{(n)},\, \widehat{A}_0^{(n)} \propto \frac{1}{\Lambda^n}. \tag{76}$$

As the space is taken to be flat in this region, we can expand the self-dual instanton (8) to provide the leading order contribution. Given that $\mu^2 = \mathcal{O}(1/\Lambda)$ then the first term in the expansion is

$$A_I^{(1)} = -\frac{i}{2}\mu^2 \sigma_{IJ}\partial_J \frac{1}{\rho^2} \propto \frac{1}{\Lambda}, \tag{77}$$

which satisfies the field equations ((58) and (59) with $H = 1$) at the linear level.

From (63) the abelian gauge potential at linear order is

$$\widehat{A}_0^{(1)} = \frac{8}{\Lambda\rho^2}, \tag{78}$$

which satisfies the final field equation ((60) with $H = 1$) at linear order.

This linear expansion is extended beyond the region $\rho \lesssim L = 1$ by taking into account the curvature of the metric. As the first order terms $A_I^{(1)}$ and $\widehat{A}_0^{(1)}$ satisfy the linearised field equations, the approach[13] is to perform a separation of variables in x_i

and z, expand in eigenfunctions of the linear operator in flat space, and then extend each eigenfunction separately into the curved region beyond $\rho \lesssim 1$. The existence of an overlap region $1/\sqrt{\Lambda} \lesssim \rho \lesssim 1$, in which the linear flat space approximation and the linear curved space approximation are both valid, allows the computation of the coefficients of the eigenfunction expansion in curved space.

The abelian potential $\widehat{A}_0^{(1)}$ satisfies the linearized field equation (60) given by

$$\partial_i \partial_i \widehat{A}_0^{(1)} + H^{1/2} \partial_z (H^{3/2} \partial_z \widehat{A}_0^{(1)}) = 0. \tag{79}$$

We can therefore extend (78) to the curved regime by writing

$$\widehat{A}_0^{(1)} = \frac{8}{\Lambda} \xi(x_I) \tag{80}$$

where $\xi(x_I)$ is a harmonic function in the four-dimensional curved space, such that in the flat regime it is given by

$$\xi \simeq \frac{1}{\rho^2} \qquad \text{for} \quad \rho \lesssim 1. \tag{81}$$

By separating variables this harmonic function can be expanded in a Laplace-Fourier expansion (Laplace expansion in r, Fourier expansion in z). In flat space there is the exact identity

$$\frac{1}{\rho^2} = \frac{1}{r^2 + z^2} = \int_0^\infty \frac{e^{-kr}}{r} \cos(kz)\, dk, \tag{82}$$

where all the momentum modes k appear in this expansion to reconstruct the function $1/\rho^2$ exactly. We can extend this expansion into the curved region by replacing it with

$$\xi = \int_0^\infty \frac{e^{-kr}}{r} \psi_{(k)}^+(z)\, dk, \tag{83}$$

where $\psi_{(k)}^\pm(z)$ are the eigenfunctions defined earlier that solve (48).

The expression (80) with ξ defined in (83) gives the exact extension of $\widehat{A}_0^{(1)}$ in the curved region and reduces to (81) in the almost flat region since, for every value of k,

$$\psi_{(k)}^+(z) \simeq \cos(kz) \qquad \text{for} \qquad z \ll 1, \tag{84}$$

as $H \simeq 1$ in this region.

A similar analysis for the gauge potential $A_I^{(1)}$ yields the result

$$A_i^{(1)} = -\frac{i}{2}\mu^2 \left(\varepsilon_{ijk} \sigma_k \partial_j \xi + \sigma_i \int_0^\infty \frac{e^{-kr}}{r} k^2 \psi_{(k)}^-(z)\, dk \right), \tag{85}$$

$$A_z^{(1)} = -\frac{i}{2}\mu^2 \sigma_i \int_0^\infty \partial_i \frac{e^{-kr}}{r} \phi_{(k)}^+(z)\, dk, \tag{86}$$

where we have defined the functions

$$\phi_{(k)}^+(z) = \partial_z \psi_{(k)}^-(z). \tag{87}$$

The expressions (80), (85) and (86) are exact identities, but only if all the momentum modes k are included. However, as we have already seen, the conformal boundary restricts the allowed momenta k to discrete values k_n. To make sense of these expressions we must therefore project to the subspace of allowed eigenfunctions to obtain

$$\xi = \sum_{n=1}^{\infty} \xi_{2n-1} \frac{e^{-k_{2n-1}r}}{r} \psi_{2n-1}(z), \tag{88}$$

$$A_i^{(1)} = -\frac{i}{2}\mu^2 \left(\varepsilon_{ijk}\sigma_k \partial_j \xi + \sigma_i \sum_{n=1}^{\infty} \xi_{2n} \frac{e^{-k_{2n}r}}{r} k_{2n}^2 \psi_{2n}(z) \right), \tag{89}$$

$$A_z^{(1)} = -\frac{i}{2}\mu^2 \sigma_i \sum_{n=0}^{\infty} \xi_{2n} \partial_i \frac{e^{-k_{2n}r}}{r} \phi_{2n}(z), \tag{90}$$

where the projection coefficients ξ_n are defined by

$$\xi_{2n-1} = \frac{1}{(\psi_{2n-1}, \psi_{2n-1})} \int_0^{\infty} (\psi_{(k)}^+, \psi_{2n-1})\, dk, \tag{91}$$

$$\xi_{2n} = \frac{1}{\langle \phi_{2n}, \phi_{2n} \rangle} \int_0^{\infty} \langle \phi_{(k)}^+, \phi_{2n} \rangle\, dk, \tag{92}$$

using the inner products (52) and (54) introduced earlier.

The discretization (88) has the following important consequence. Within the linear approximation, the large distance decay of ξ is now exponential in r rather than algebraic, because $k_1 > 0$. Thus the conclusion from the linear analysis in curved space is that at large three-dimensional distance, $r \gtrsim 1$, all terms decay exponentially, except the algebraic decay associated with the pion field. Explicitly,

$$\begin{aligned} A_z^{(1)} &= \frac{i\xi_0\mu^2}{2} \frac{\sigma_i x_i}{r^3} \phi_0(z) + \mathcal{O}\left(\frac{e^{-k_2 r}}{r}\right), \\ A_i^{(1)} &= \mathcal{O}\left(\frac{e^{-k_1 r}}{r}\right), \qquad \widehat{A}_0^{(1)} = \mathcal{O}\left(\frac{e^{-k_1 r}}{r}\right), \end{aligned} \tag{93}$$

where we recall that k_1 and k_2 are the masses of the lightest vector meson and the lightest axial vector meson respectively. This linear result was first obtained using a slightly different, though equivalent, analysis[34].

As $\widehat{A}_0$ is the field dual to the baryon current of the boundary theory, the conclusion from this linear analysis is that the baryon form factors decay exponentially. However, this conclusion is incorrect because the above linear result cannot be extended to arbitrarily large values of the radius r. The linear results do have a region of validity, but this region does not include arbitrarily large r, since nonlinear terms dominant over the linear result (93). This has been the source of several erroneous calculations and conclusions in the literature.

To derive the correct large r behaviour of the fields requires a nonlinear analysis[13]. For this, we can ignore all terms that decay exponentially with r, as we are interested in the details of the algebraic decay. Thus we may set $A_i^{(1)} = \widehat{A}_0^{(1)} = 0$,

upon neglecting the exponential terms. To proceed, we keep the leading order terms in a $1/r$ expansion at each order in a $1/\Lambda$ expansion.

Starting with the linear terms in $1/\Lambda$

$$A_z^{(1)} = \frac{i\xi_0\mu^2}{2}\,\frac{\sigma_i x_i}{r^3}\,\phi_0, \qquad A_i^{(1)} = 0, \qquad \widehat{A}_0^{(1)} = 0, \tag{94}$$

we solve the field equations at each order in $1/\Lambda$. The first non-zero term in A_i occurs at second order and is found to be

$$A_i^{(2)} = -\frac{i}{16}\xi_0^2\mu^4\varepsilon_{ijk}\frac{x_j}{r^6}\sigma_k(4\psi_0^2 - \pi^2), \tag{95}$$

whereas the first non-zero term in $\widehat{A}_0$ occurs at fourth order and is given by

$$\widehat{A}_0^{(4)} = -\frac{2\xi_0^3\mu^6}{\Lambda r^9}\left(\psi_0^4 - 6\left(\frac{\pi}{2}\right)^2\psi_0^2 + 5\left(\frac{\pi}{2}\right)^4\right). \tag{96}$$

These expressions provide the leading order large r behaviour of all the fields and their relation to the small self-dual instanton approximation. Note the significant difference in the rate of decay of the field $\widehat{A}_0$ in the r and z directions, as it decays as $\mathcal{O}(1/r^9)$ for large r but decays only as $\mathcal{O}(1/z)$ for large z. Recall that the faster decay along the r-axis compared to the z-axis was already noted in the earlier numerical results.

The above results imply the existence of a new large scale, at which the behaviour of the A_i and $\widehat{A}_0$ components are dominated by nonlinear terms. The new scale is where the linear terms in the $1/\Lambda$ expansion of A_i and $\widehat{A}_0$ (including the exponentially decaying terms) are comparable to the higher order terms, that is, $A_i^{(1)} \sim A_i^{(2)}$, $\widehat{A}_0^{(1)} \sim \widehat{A}_0^{(4)}$. From above this is equivalent to

$$\frac{e^{-k_1 r}}{\Lambda r} \sim \frac{1}{\Lambda^2 r^5},\ \frac{1}{\Lambda^4 r^9}, \tag{97}$$

so a new length scale appears at $r \sim \log\Lambda$, or more generally $r \sim L\log\Lambda$, if we reinstate the scale L. Note that this is a large scale for large Λ. It is the scale beyond which the asymptotic fields with algebraic decay are applicable to describe the tail of the holographic Skyrmion. The size of the holographic Skyrmion is therefore a complicated issue, even though the size of the approximating self-dual instanton is a known small value.

In summary, there are three important scales for the holographic Skyrmion. The scale of the self-dual instanton, $L/\sqrt{\Lambda}$, the radius of curvature L, and the new scale of order $L\log\Lambda$. The various approximations discussed above are valid in different regions, some of which are contiguous and therefore allow the different approximations to be related. These different regions correspond to the treatment of space as flat or curved and the analysis of the partial differential equations at

the linear or nonlinear level. Schematically, we may summarise the situation as:

$$\begin{aligned} 0 < \rho &\lesssim L/\sqrt{\Lambda}, && \text{flat and nonlinear} \\ L/\sqrt{\Lambda} &\lesssim \rho \lesssim L, && \text{flat and linear} \\ L &\lesssim \rho \lesssim L\log\Lambda, && \text{curved and linear} \\ L\log\Lambda &\lesssim \rho && \text{curved and nonlinear.} \end{aligned} \tag{98}$$

The appearance of the final region is a slightly unusual feature that is a consequence of the fact that the nonlinear terms dominate over the linear terms at large radius.

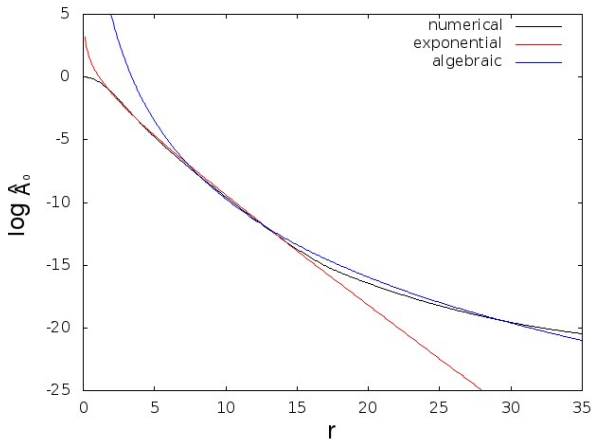

Fig. 6. For the holographic Skyrmion with $\Lambda = 2$, the plot displays $\log \widehat{A}_0$ against r along the r-axis (black curve). The red curve is the exponential decay predicted by the linear approximation in curved space and the blue curve is the algebraic decay predicted by the nonlinear approximation in curved space. Exponential decay is a good approximation in the region $1 \lesssim r \lesssim 15$ and algebraic decay is a good approximation in the region $r \gtrsim 8$

To provide numerical evidence to support the above analytic calculations, concerning the applicability of the linear and nonlinear descriptions of the holographic Skyrmion tail in different regions, requires a value of Λ that is of order one. The relevant regime from the physical point of view is large Λ, but as the three length scales involved are of order $1/\sqrt{\Lambda}$, 1, $\log\Lambda$, this gives a separation of scales that is difficult to encompass within a single numerical simulation. By considering parameter values of Λ that are of order one, we can bring these three length scales closer together, so that all three are simultaneously accessible within a feasible simulation.

Applying the numerical scheme described earlier, the holographic Skyrmion is computed for $\Lambda = 2$. To examine the soliton tail, we plot $\log \widehat{A}_0$ against r (along the r-axis) in Figure 6. Also included in this plot is the leading order exponential decay predicted by the linear analysis, namely $\widehat{A}_0 = \alpha_1 e^{-k_1 r}/r$, and the leading order algebraic decay predicted by the nonlinear analysis, $\widehat{A}_0 = \alpha_2/r^9$, where $\alpha_{1,2}$

are constants. It can be seen that exponential decay is a good approximation in the region $1 \lesssim r \lesssim 15$, where the linear regime is valid, and algebraic decay is a good approximation in the region $r \gtrsim 8$, which is the nonlinear regime. The slight discrepancy between the algebraic form and the numerical result at large r is due to the finite boundary at $r = r_\star = 40$, which is not far beyond the range plotted in this figure. This numerical result is in good agreement with the analytic calculations.

The nonlinear tail fields with algebraic decay satisfy some model independent form factor relations[35], resolving an earlier puzzle that the linear tail fields with exponential decay violate these universal relations. Once the correct algebraic decay is recognized the puzzle evaporates, as it was simply a consequence of applying a linear result beyond its region of validity. The algebraic decay of the holographic Skyrmion fields was first discovered by Cherman and Ishii[36], who performed a large r expansion to obtain the asymptotic fields. However, they were only able to implement their approach by introducing a UV cutoff, with an associated singularity in the limit as this cutoff is removed: prompting them to speculate on possible resolutions that included holographic renormalization and boundary counterterms. In fact, their required UV cutoff is merely a gauge artifact that is a consequence of a gauge choice that is incompatible with the holographic boundary conditions. This issue arose because that they were unable to relate their asymptotic expansion directly to the flat space self-dual instanton approximation, and hence a vital piece of information was absent and led to the introduction of the spurious UV cutoff.

The numerical computation of the holographic 1-Skyrmion in the Sakai-Sugimoto model is possible because the $SO(3)$ symmetry of this solution reduces the calculation to an effective two-dimensional problem. However, holographic multi-Skyrmions and solutions with finite density are unlikely to have any continuous symmetries, so numerical field theory computations would require a fully four-dimensional computation that is beyond current capabilities.

The construction of holographic Skyrmions at finite density is a crucial aspect for understanding the important issue of dense QCD. In the limit of a large number of colours, which is the regime of holographic QCD, cold nuclear matter becomes a crystalline solid, although the details of this are still to be understood. It should be possible to capture this behaviour via a holographic Skyrmion description within the Sakai-Sugimoto model. However, the lack of numerical computations has led to various approximate methods being employed to describe this phase, as follows.

Calorons, which are flat space self-dual Yang-Mills instantons with a periodic direction, can split into monopole constituents if the period is smaller than the instanton size. This fact, together with a point particle approximation, has led to the suggestion[14] that the appropriate holographic Skyrmion crystal consists of pairs of dyons with opposite charges arranged in a salt-like configuration. It is argued that, with increasing density, this dyonic salt arrangement turns into a cubic crystal of half-instantons that is dual to the Skyrme crystal described earlier. In a different study, making use of approximations involving flat space calorons and dilute instantons, it has been proposed[15,16] that with increasing density a series

of transitions takes place, dubbed baryonic popcorn, where the three-dimensional crystal develops additional layers in the holographic direction. Unfortunately, even classical field theory computations are not yet available to test these ideas in the Sakai-Sugimoto model. In the following section we review holographic Skyrmions within a low-dimensional analogue[17] of the Sakai-Sugimoto model, where analogues of these issues can be studied both analytically and numerically.

5. A low-dimensional analogue of holographic Skyrmions

The bulk theory of interest in this section is defined in a three-dimensional spacetime with negative curvature, and is an $O(3)$ sigma model with a baby Skyrme term that plays the role of the Chern-Simons term in the Sakai-Sugimoto model. It is well-known that instantons in planar sigma models are natural low-dimensional analogues of Yang-Mills instantons. If the coefficient of the baby Skyrme term is small then the holographic Skyrmion in this low-dimensional theory has a small size and may be approximated by an instanton of the flat space sigma model. The advantage of the lower-dimensional theory is that numerical simulations of holographic multi-Skyrmions and finite density solutions can be performed and compared with predictions using flat space instanton approximations. In particular, analogues of dyonic salt and baryonic popcorn configurations have been found and analysed[17] and the results provide evidence to support the validity of these ideas within the Sakai-Sugimoto model.

The bulk spacetime for the low-dimensional theory is given by the three-dimensional metric (39) and (40) with $D = 1$. We apply the same index notation as in the previous section, so that $g_{\Gamma\Delta}$ denotes the components of this three-dimensional metric with spacetime coordinates t, x, z. The scalar curvature is

$$R = -\frac{(z^2+4)}{2(1+z^2)^{3/2}}, \tag{99}$$

so again the spacetime has finite negative curvature.

The action of the massless $O(3)$ baby Skyrme model in the above spacetime is

$$S = \int \left(\frac{1}{2} g^{\Gamma\Delta} \partial_\Gamma \boldsymbol{\phi} \cdot \partial_\Delta \boldsymbol{\phi} + \frac{1}{4\Lambda^2} g^{\Gamma\Delta} g^{\Sigma\Xi} (\partial_\Gamma \boldsymbol{\phi} \times \partial_\Sigma \boldsymbol{\phi}) \cdot (\partial_\Delta \boldsymbol{\phi} \times \partial_\Xi \boldsymbol{\phi}) \right) \sqrt{-g}\, dx\, dz\, dt, \tag{100}$$

where $\boldsymbol{\phi} = (\phi_1, \phi_2, \phi_3)$ is a three-component unit vector. The first term in the above action is that of the $O(3)$ sigma model and the second term is the baby Skyrme term[37], with a constant coefficient $1/\Lambda^2$. We shall be interested in the regime of large Λ, this constant playing the role of the 't Hooft coupling in the Sakai-Sugimoto model, hence the use of the same symbol to denote it.

The associated static energy is

$$E = \frac{1}{2} \int \left(\frac{1}{H} |\partial_x \boldsymbol{\phi}|^2 + H\, |\partial_z \boldsymbol{\phi}|^2 + \frac{1}{\Lambda^2} |\partial_x \boldsymbol{\phi} \times \partial_z \boldsymbol{\phi}|^2 \right) \sqrt{H}\, dx\, dz, \tag{101}$$

and the boundary condition is that $\boldsymbol{\phi} \to (0,0,1)$ as $x^2 + z^2 \to \infty$. This theory has holographic Skyrmions that share many analogous features to those in the Sakai-Sugimoto model. The analogue of the baryon number is the integer-valued topological charge

$$B = -\frac{1}{4\pi} \int \boldsymbol{\phi} \cdot (\partial_x \boldsymbol{\phi} \times \partial_z \boldsymbol{\phi})\, dx\, dz, \tag{102}$$

which defines the instanton number of the planar sigma model.

The simple inequality

$$\left| \frac{1}{\sqrt{H}} \partial_x \boldsymbol{\phi} \pm \sqrt{H} \boldsymbol{\phi} \times \partial_z \boldsymbol{\phi} \right|^2 \geq 0, \tag{103}$$

combined with the fact that $H \geq 1$, yields the energy bound $E \geq 4\pi |B|$.

In flat space without a baby Skyrme term, that is, in the $\Lambda \to \infty$ limit with $H = 1$, this inequality is attained by the instanton solutions of the $O(3)$ sigma model[38]. To write these instanton solutions explicitly it is convenient to use the equivalent formulation of the $O(3)$ sigma model in terms of the $\mathbb{CP}^1$ sigma model, by defining the Riemann sphere coordinate $W = (\phi_1 + i\phi_2)/(1 - \phi_3)$, obtained by stereographic projection of $\boldsymbol{\phi}$. In terms of this variable, instanton solutions are given by W a holomorphic function of $\zeta = x + iz$. The instanton solutions with finite $B > 0$ are given by $W(\zeta)$ a rational function of degree B, where the degree of the numerator is larger than that of the denominator in order to satisfy the above boundary condition. Taking into account the global $U(1)$ symmetry associated with the phase of W, this leaves an instanton moduli space of dimension $4B - 1$.

The radially symmetric sigma model instanton with topological charge B and centre at the origin is given by $W = (\zeta/\mu)^B$, where the positive real constant μ is the arbitrary size of the instanton.

In the large Λ regime the sigma model term dominates over the baby Skyrme term and it is reasonable to approximate the holographic Skyrmion by a sigma model instanton: imitating the similar instanton approximation in the Sakai-Sugimoto model. Here too, the curvature acts to shrink the instanton size whereas the baby Skyrme term produces a contribution to the energy that increases with decreasing instanton size and balances the curvature contribution to yield a preferred small size for the instanton.

Again, this can be made explicit by introducing the rescaled variables $\widetilde{x} = x\sqrt{\Lambda}$ and $\widetilde{z} = z\sqrt{\Lambda}$, with $\widetilde{H}$ denoting $H(\widetilde{z}/\sqrt{\Lambda})$. In terms of these variables the energy (101) becomes

$$E = \frac{1}{2} \int \left(\widetilde{H}^{-1/2} \left| \partial_{\widetilde{x}} \boldsymbol{\phi} \right|^2 + \widetilde{H}^{3/2} \left| \partial_{\widetilde{z}} \boldsymbol{\phi} \right|^2 + \frac{1}{\Lambda} \widetilde{H}^{1/2} |\partial_{\widetilde{x}} \boldsymbol{\phi} \times \partial_{\widetilde{z}} \boldsymbol{\phi}|^2 \right) d\widetilde{x}\, d\widetilde{z}. \tag{104}$$

Expanding this energy as a series in $1/\Lambda$ yields

$$E = \frac{1}{2}\int \left\{ |\partial_{\widetilde{x}}\boldsymbol{\phi}|^2 + |\partial_{\widetilde{z}}\boldsymbol{\phi}|^2 \ + \frac{1}{\Lambda}\left(\frac{1}{4}\widetilde{z}^2(3|\partial_{\widetilde{z}}\boldsymbol{\phi}|^2 - |\partial_{\widetilde{x}}\boldsymbol{\phi}|^2) + |\partial_{\widetilde{x}}\boldsymbol{\phi}\times\partial_{\widetilde{z}}\boldsymbol{\phi}|^2\right) + \mathcal{O}\left(\frac{1}{\Lambda^2}\right)\right\} d\widetilde{x}\, d\widetilde{z}. \tag{105}$$

The leading order term in this static energy is that of the planar flat space $O(3)$ sigma model, in rescaled variables. Instantons minimize this contribution, which is given by $4\pi B$. The remaining terms provide an energy function on the instanton moduli space and in each topological sector the holographic Skyrmion is best approximated by the charge B instanton that minimizes this energy. Both the curvature and the baby Skyrme term contributions can already be seen at the $\mathcal{O}(1/\Lambda)$ level in (105). Balancing these contributions yields a preferred instanton size that is propotional to $1/\sqrt{\Lambda}$ in unscaled coordinates.

The holographic 2-Skyrmion can be studied within the instanton approximation by considering a two-dimensional subset of the 2-instanton moduli space that includes radial 2-instantons. Explicitly, the relevant charge 2 instantons have the form

$$W = \frac{\zeta^2 - a^2}{\mu^2}, \tag{106}$$

where μ and a are real parameters. This describes two instantons separated along the non-holographic direction with positions $(x, z) = (\pm a, 0)$ and μ determines their equal size. Radial solutions correspond to the choice $a = 0$. Calculating the energy (101) of this field reveals that it has minimum at a non-zero value of a that is $\mathcal{O}(1/\sqrt{\Lambda})$. Furthermore, this calculation reveals that the separation $2a$ between the two instantons is approximately equal to the size μ of the 2-instanton. In other words, it predicts that the holographic 2-Skyrmion should closely resemble two touching holographic single Skyrmions.

The main advantage of the low-dimensional model is that it is possible to obtain full numerical solutions of the nonlinear field theory, because the static problem is only two-dimensional and is therefore within the reach of modest computational resources. The results[17] of field theory computations are reproduced in Figure 7, for the parameter value $\Lambda = 100$. The $B = 1$ holographic Skyrmion is displayed in the left image and the $B = 2$ holographic Skyrmion in the right image. The plot shows ϕ_3, as this gives a good pictorial representation of these low-dimensional holographic Skyrmions.

It can be seen that the $B = 1$ solution has an approximate radial symmetry and a size that is roughly $1/\sqrt{\Lambda} = 0.1$, in agreement with the instanton approximation. The accuracy of the instanton approximation is confirmed by an energy comparison, as the numerical field theory computation yields a value $E = 4\pi \times 1.0148$ to be compared with the energy of the instanton approximation $E = 4\pi \times 1.0154$.

The $B = 2$ solution has an energy $E = 8\pi \times 1.0105$, so this is a bound state of two holographic 1-Skyrmions. Note that the binding energy per Skyrmion is

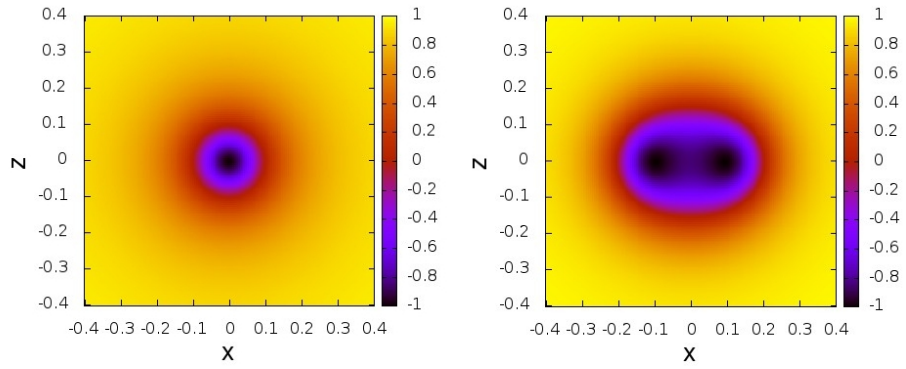

Fig. 7. A plot of ϕ_3 for the holographic 1-Skyrmion (left image) and the holographic 2-Skyrmion (right image).

less than 0.5% of the single Skyrmion energy, illustrating the fact that holographic models based on perturbations around BPS systems can yield the kind of small binding energies found in real nuclei. As predicted by the instanton approximation, the holographic 2-Skyrmion does not have (even approximate) radial symmetry but resembles two single holographic Skyrmions separated along the non-holographic direction, with a separation that is close to the diameter of a single holographic Skyrmion.

The energy of the 2-instanton approximation (106) is minimized for the instanton parameters $a = 0.095$ and $\mu = 0.18$ with an energy that is only 0.03% above the field theory computation. As expected from this result, a plot of ϕ_3 using this instanton approximation produces an image that is essentially identical to the right image displayed in Figure 7.

The validity of the 2-instanton approximation (106) also reveals that the most attractive arrangement of two holographic Skyrmions corresponds to a relative internal phase of π between the two constituent Skyrmions. The argument for this follows from the product ansatz for two fields W_1 and W_2, given by

$$W = \frac{W_1 W_2}{W_1 + W_2}. \tag{107}$$

Consider the above product ansatz for two instantons of equal size, with a relative phase χ and positions $\pm a$ along the x-axis. Explicitly,

$$W_1 = \frac{\zeta - a}{\nu}, \quad W_2 = e^{i\chi}\frac{\zeta + a}{\nu}, \quad \text{producing} \quad W = \frac{e^{i\chi}(\zeta^2 - a^2)}{\nu(\zeta(e^{i\chi}+1) + a(e^{i\chi}-1))}. \tag{108}$$

This field matches the 2-instanton expression (106) if $e^{i\chi} = -1$ and $\nu = \mu^2/(2a)$, hence the relative internal phase is $\chi = \pi$. Thus two holographic Skyrmions are in the attractive channel if they are exactly out of phase.

Numerical field theory computations for holographic Skyrmions with larger values of B yield a string of B single holographic Skyrmions that are touching and

aligned along the non-holographic direction with alternating internal phases, so that all neighbouring pairs are exactly out of phase. This is the expected result given the structure of the holographic 2-Skyrmion and the fact that the curvature favours holographic Skyrmions located along the line $z = 0$.

Finally, we turn our attention to low-dimensional holographic Skyrmions with finite density. As mentioned earlier, in the Sakai-Sugimoto model the study of holographic Skyrmions at finite density has attracted some recent attention in attempts to understand dense QCD within a holographic setting. As numerical field theory simulations are currently not tractable, various approximations have been applied to make progress on this topic. However, even the flat space self-dual Yang-Mills instanton approximation is difficult to apply to this situation because the relevant self-dual instanton is not available in explicit form for periodic boundary conditions in multiple dimensions. The low-dimensional theory is a more tractable proposition, not only because numerical field theory computations can be performed, but also because there are simple explicit formulae for the relevant flat space sigma model periodic instantons.

To numerically compute holographic Skyrmions at finite density, the non-holographic direction is restricted to the range $-l \leq x \leq l$ and periodic boundary conditions are imposed. The integral expression (102) for the baryon number, with the range of integration now restricted to the strip $(x, z) \in [-l, l] \times (-\infty, \infty)$, is still integer-valued and defines the finite density $\rho = B/(2l)$.

Computing the energy per baryon E/B as a function of the density ρ for a chain of holographic Skyrmions with alternating internal phases yields an optimal density of $\rho = 2.8$, at which the energy per baryon is $E/B = 4\pi \times 1.0097$. The left image in Figure 8 displays ϕ_3 for this optimal density chain.

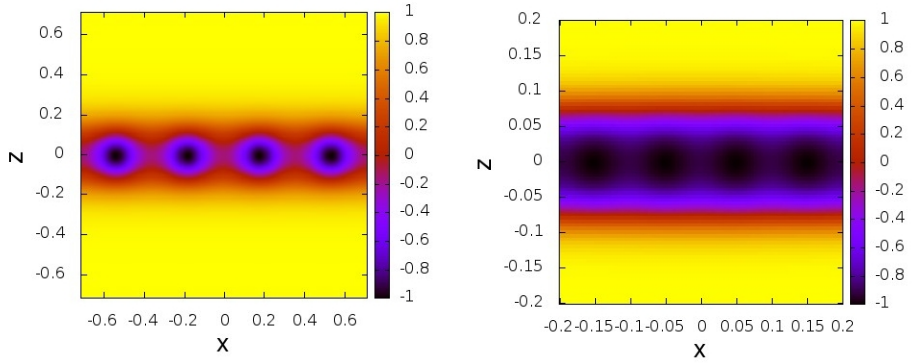

Fig. 8. A plot of ϕ_3 for a chain with the optimal density $\rho = 2.8$ (left image) and the density $\rho = 10$ (right image).

The chain solution at high density is displayed in the right image in Figure 8,

which corresponds to a density $\rho = 10$: more than three times the optimal density. At such a high density each holographic Skyrmion splits into a kink anti-kink pair separated along the holographic direction and the holographic Skyrmions lose their individual identities. The formation of this almost homogeneous structure in the non-holographic direction is the lower-dimensional analogue of the appearance of monopole constituents for calorons and has been discussed previously for instantons of the $O(3)$ sigma model in flat space[39,40,41]. A configuration of this type is therefore a low-dimensional analogue of the dyonic salt arrangement[14].

Beyond the optimal density, the energy per baryon of the chain grows rapidy with increasing density. The baryonic popcorn idea[15,16] suggests that there will be a critical density beyond which it is energetically preferable for the single chain to split into a pair of chains via a pop into the holographic direction. Such double chains can also be computed numerically and an example with density $\rho = 10$ is displayed in the left image in Figure 9. The phase of the holographic Skyrmions alternates within each chain and two holographic Skyrmions that lie above each other in different chains are also exactly out of phase, to produce maximal attraction between all neighbouring pairs. The obvious generalization to multiple chains is also realized and a triple chain example with density $\rho = 20$ is shown in the right image in Figure 9.

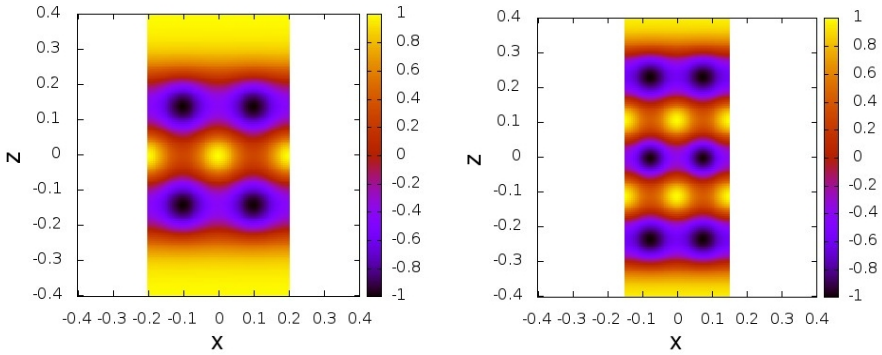

Fig. 9. A plot of ϕ_3 for the double chain with density $\rho = 10$ (left image) and the triple chain with density $\rho = 20$ (right image).

Flat space sigma model periodic instanton solutions can be used to study the above finite density configurations. The starting point is the periodic sigma model solution[39]

$$W = \nu \sin(\pi\rho\zeta), \tag{109}$$

that describes an instanton chain in which there are instantons located along the x-axis with a distance $1/\rho$ between neighbouring instantons that are exactly out of phase. The real parameter ν controls the size of each instanton, which is given

by $1/(\nu\pi\rho)$ in the dilute regime where the instanton size is small compared to $1/\rho$. Once the instanton size is comparable to $1/\rho$ the instantons lose their individual identities and as the size increases further they split into kink anti-kink constituents and the configuration tends towards the homogeneous state. This instanton chain can be used to approximate the holographic Skyrmion chain by minimizing the energy (101) of the field (109) over the parameter ν for each fixed density ρ.

Multiple chains of instantons can be constructed by using the product ansatz (107) with constituent fields obtained by translation of the single chain (109). For example, a double instanton chain is produced from the constituents

$$W_1 = \nu \sin(\pi\rho(\zeta - i\delta)/2), \qquad W_2 = -\nu \sin(\pi\rho(\zeta + i\delta)/2). \tag{110}$$

The energy (101) can then be minimized over the scale ν and the distance 2δ between the chains in the holographic direction, to yield the instanton approximation to the double chain of holographic Skyrmions.

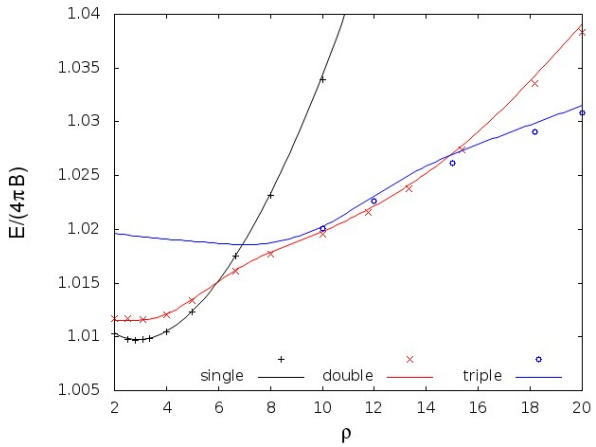

Fig. 10. A plot of $E/(4\pi B)$ against density ρ for the single chain, double chain and triple chain. Data points are the numerical solutions from field theory simulations and curves are sigma model instanton approximations.

In Figure 10 the data points represent E/B, in units of 4π, against the density ρ for the numerical field theory single, double and triple chain solutions (marked by $+, \times, \circ$ respectively). The curves show the corresponding instanton chain approximations (black, red and blue curves for single, double and triple chains respectively) and are in excellent agreement with the field theory computations.

The optimal density corresponds to the critical value of the chemical potential at which there is a first order phase transition to an equilibrium density of holographic Skyrmions, this being the analogue of the nuclear matter phase transition in QCD. Once the density is greater than about twice the optimal density, the double

chain has a lower energy than the single chain. This confirms the analogue of baryonic popcorn in the low-dimensional model. In particular, in the low-dimensional theory the popcorn phenomenon takes place at a density below that at which the holographic Skyrmions split into constituents, so this popcorn is not salted. As expected from the popcorn phenomenon, a triple chain is energetically preferred over a double chain for sufficiently high density. These results suggest that as the density is increased further then the number of chains increases and eventually the configuration begins to resemble a portion of a two-dimensional lattice rather than the one-dimensional chain that arises at the optimal density. This is exactly the phenomenon predicted by the baryonic popcorn idea[15,16].

The results in the low-dimensional theory confirm that instantons can provide good approximations to holographic Skyrmions, multi-Skyrmions and finite density solutions. This provides further support for the use of self-dual Yang-Mills instantons in approximating holographic Skyrmions in the Sakai-Sugimoto model. Furthermore, analogues of dyonic salt and baryonic popcorn configurations provide further evidence for their relevance in the study of holographic Skyrmions at finite density.

6. Conclusion

Ideas from holography and string theory have produced some interesting new twists regarding the traditional description of baryons in terms of Skyrmions. One new avenue for future research that follows from a holographic approach is the extension of the Skyrme model of pions to include other vector mesons in a way that improves the comparison with nuclear binding energies without introducing any additional free parameters into the theory. In Section 3 we reviewed a simple version of this technique, based on flat space holography, that yields some encouraging imitial results. To date, multi-Skyrmions in the extended theory have only been studied for low baryon numbers using the instanton approximation. To extend these results to higher baryon numbers, and also to check the assumed symmetries and accuracy of the instanton approximation, it will be necessary to perform full field numerical simulations of the extended theory. This is a computational challenge because of the significant increase in both the number of degrees of freedom and the number of terms in the energy, in comparison to the standard Skyrme model of pions alone.

The second avenue for future research is the computation of holographic multi-Skyrmions in the bulk Sakai-Sugimoto model, together with finite density solutions. In section 4 we reviewed the computation of the single holographic Skyrmion within this model, but this relies on the $SO(3)$ symmetry of this solution. Extending this computation beyond the single baryon sector, where a fully four-dimensional numerical calculation is required, is a major task. However, the results from such an investigation would certainly be of significant interest.

In the study of baryonic popcorn in the Sakai-Sugimoto model it has been proposed that multiple chains have a zig-zag structure[15,16]. This requires that the

optimal separation for two holographic Skyrmions is much greater than the size of a single holographic Skyrmion. In the low-dimensional analogue theory reviewed in section 5, this is not the case, so it is not surprising that zig-zag patterns fail to emerge in that theory. The baby Skyrme term provides a low-dimensional analogue of the Chern-Simons term in the Sakai-Sugimoto model, but an alternative is to couple a vector meson to the sigma model topological current, as studied in flat space[42]. It might be of interest to investigate this possibility and, in particular, to see if a zig-zag structure appears in this alternative version of low-dimensional holographic Skyrmions.

Finally, the issue of quantization of holographic Skyrmions must be addressed, once the classical solutions are available for multi-baryons. Even within a zero mode quantization, the quantum contributions to the energy from spin and isospin are likely to be sensitive to the method used to fix the energy and length units. However, these quantum corrections must be small if an accurate fit to nuclear binding energies is to be achieved, because these contributions vanish for the ground state of ^{4}He, which is a spin zero and isospin zero state.

Acknowledgements

The material reviewed in sections 4 and 5 of this review article is based on joint work with Stefano Bolognesi. The research of the author is supported by the EPSRC grant EP/K003453/1 and the STFC grant ST/J000426/1.

References

1. T. H. R. Skyrme, *Nucl. Phys.* **31**, 556 (1962).
2. N. S. Manton and P. M. Sutcliffe, *Topological Solitons*, Cambridge University Press (2004).
3. E. Witten, *Nucl. Phys.* **B223**, 422 (1983); *ibid* **B223**, 433 (1983).
4. *The Multifaceted Skyrmion*, Eds. G. E. Brown and M. Rho, World Scientific Publishing (2010).
5. R. A. Battye and P. M. Sutcliffe, *Phys. Rev. Lett.* **86**, 3989 (2001); *Rev. Math. Phys.* **14**, 29 (2002).
6. G. S. Adkins, *Phys. Rev.* **D33**, 193 (1986).
7. U. G. Meissner and I. Zahed, *Phys. Rev. Lett.* **56**, 1035 (1986).
8. M. Bando, T. Kugo, S. Uehara, K. Yamawaki and T. Yanagida, *Phys. Rev. Lett.* **54**, 1215 (1985).
9. M. Bando, T. Kugo and K. Yamawaki, *Phys. Reports* **164**, 217 (1988).
10. M. Harada and K. Yamawaki, *Phys. Reports* **381**, 1 (2003).
11. T. Sakai and S. Sugimoto, *Prog. Theor. Phys.* **113**, 843 (2005).
12. M. F. Atiyah and N. S. Manton, *Phys. Lett.* **B222**, 438 (1989); *Commun. Math. Phys.* **153**, 391 (1993).
13. S. Bolognesi and P. M. Sutcliffe, *JHEP* **1401**, 078 (2014).
14. M. Rho, S.-J. Sin and I. Zahed, *Phys. Lett.* **B689**, 23 (2010).
15. V. Kaplunovsky, D. Melnikov and J. Sonnenschein, *JHEP* **1211**, 047 (2012).
16. V. Kaplunovsky and J. Sonnenschein, *JHEP* **1404**, 022 (2014).
17. S. Bolognesi and P. M. Sutcliffe, *J. Phys.* **A47**, 135401 (2014).

18. L. D. Faddeev, *Lett. Math. Phys.* **1**, 289 (1976).
19. L. Castillejo, P. S. J. Jones, A. D. Jackson, J. J. M. Verbaarschot and A. Jackson, *Nucl. Phys.* **A501**, 801 (1989).
20. M. Kugler and S. Shtrikman, *Phys. Lett.* **B208**, 491 (1988); *Phys. Rev.* **D40**, 3421 (1989).
21. D. T. J. Feist, P. H. C. Lau and N. S. Manton, *Phys. Rev.* **D87**, 085034 (2013).
22. M. F. Atiyah, N. J. Hitchin, V. G. Drinfeld and Yu. I. Manin, *Phys. Lett.* **A65**, 185 (1978).
23. R. A. Leese and N. S. Manton, *Nucl. Phys.* **A572**, 575 (1994).
24. M. A. Singer and P. M. Sutcliffe, *Nonlinearity* **12**, 987 (1999).
25. P. M. Sutcliffe, *Proc. R. Soc. Lond.* **A460**, 2903 (2004).
26. N. S. Manton and P. M. Sutcliffe, *Phys. Lett.* **B342**, 196 (1995).
27. P. M. Sutcliffe, *JHEP* **1008**, 019 (2010).
28. P. M. Sutcliffe, *JHEP* **1104**, 045 (2011).
29. D. K. Hong, M. Rho, H-U. Yee, P. Yi *Phys.Rev.* **D76**, 061901 (2007).
30. H. Hata, T. Sakai, S. Sugimoto and S. Yamato, *Prog. Theor. Phys.* **117**, 1157 (2007).
31. T. Sakai and S. Sugimoto, *Prog. Theor. Phys.* **114**, 1083 (2005).
32. E. Witten, *Phys. Rev. Lett.* **38**, 121 (1977).
33. P. Forgacs and N. S. Manton, *Commun. Math. Phys.* **72**, 15 (1980).
34. K. Hashimoto, T. Sakai and S. Sugimoto, *Prog. Theor. Phys.* **120**, 1093 (2008).
35. A. Cherman, T. D. Cohen and M. Nielsen, *Phys. Rev. Lett.* **103**, 022001 (2009).
36. A. Cherman and T. Ishii, *Phys. Rev.* **D86**, 045011 (2012).
37. B. M. A. G. Piette, B. J. Schroers and W. J. Zakrzewski, *Z. Phys.* **C65**, 165 (1995).
38. W. J. Zakrzewski, *Low Dimensional Sigma Models*, Bristol, Institute of Physics Publishing, 1989.
39. F. Bruckmann, *Phys. Rev. Lett.* **100**, 051602 (2008).
40. M. Eto, T. Fujimori, Y. Isozumi, M. Nitta, K. Ohashi, K. Ohta and N. Sakai, *Phys. Rev.* **D73**, 085008 (2006).
41. D. Harland, *J. Math. Phys.* **50**, 122902 (2009).
42. D. Foster and P.M. Sutcliffe, *Phys. Rev.* **D79**, 125026 (2009).